https://doi.org/10.3799/dqkx.2025.051

琼东南盆地松南低凸起晚三叠世花岗岩潜山形成和演化

杨海长[1],唐华风[2],纪　沫[1*],田志文[2],高有峰[2]

1. 中海油研究总院有限责任公司,北京 100028
2. 吉林大学地球科学学院,吉林长春 130061

摘　要: 为了进一步研究松南低凸起花岗岩潜山演化过程,对 Y8-A 井基底二长花岗岩进行年代学、主微量、Sr-Nd-Pb-Hf同位素、磷灰石裂变径迹和锆石(U-Th)/He分析 .LA-ICP-MS 锆石 U-Pb 定年结果为 235.6±4.8 Ma,基性岩脉 $^{40}Ar/^{39}Ar$ 坪年龄为 141.57±0.63 Ma. 花岗岩主微量元素特征表明其为高钾钙碱性、过铝质 S 型花岗岩 . 花岗岩($^{87}Sr/^{86}Sr$)$_i$ 比值为 0.707 93～0.709 44,$\varepsilon_{Nd}(t)$值为－4.45～－6.39,$\varepsilon_{Hf}(t)$值为－5.6～1.5. 磷灰石裂变径迹年龄为 66.3±5.6 Ma,锆石(U-Th)/He 单颗粒年龄为(82.05±1.99)～(45.93±1.14) Ma. 综合研究表明,二长花岗岩形成于印支与华南碰撞拼合后的后碰撞背景,热史反演结果表明花岗岩潜山的演化可分为侵位冷凝、缓慢冷却、较快冷却、近地表剥露和沉降埋藏 5 个阶段 .

关键词: 琼东南盆地;松南低凸起;花岗岩潜山;岩石成因;构造演化;岩石学;年代学 .

中图分类号: P581　　**文章编号:** 1000－2383(2025)06－2124－20　　**收稿日期:** 2024-08-20

Formation and Evolution of the Late Triassic Granite Buried Hill in the Songnan Low Uplift, Qiongdongnan Basin

Yang Haizhang[1], Tang Huafeng[2], Ji Mo[1*], Tian Zhiwen[2], Gao Youfeng[2]

1. *China National Offshore Oil Corporation* (*CNOOC*) *Research Institute Co.*, *Ltd.*, *Beijing* 100028, *China*
2. *College of Earth Sciences*, *Jilin University*, *Changchun* 130061, *China*

Abstract: To further study the evolution process of the Songnan Low Uplift granite buried hill, the basement monzogranite in well Y8-A are analysed by chronology, major and trace, Sr-Nd-Pb-Hf isotopes, apatite fission track, and zircon (U-Th)/He methods. LA-ICP-MS zircon U-Pb dating is 235.6±4.8 Ma. The mafic dikes $^{40}Ar/^{39}Ar$ flateau age is 141.57±0.63 Ma. These granites belong to high potassium calc alkaline and peraluminous S-type granite. Their ($^{87}Sr/^{86}Sr$)$_i$, $\varepsilon_{Nd}(t)$, and $\varepsilon_{Hf}(t)$ values are 0.707 93－0.709 44, －4.45 to －6.39, and -－5.6 to 1.5, respectively. The apatite fission track age is 66.3±5.6 Ma, and the single zircon (U-Th) /He particle age ranges from (82.05±1.99) to (45.93±1.14) Ma. The comprehensive study shows that the monzogranite was formed in the post-collision background after the collision between Indochina and South China. The thermal history inversion results show that the evolution of granite buried hill can be divided into five stages:emplacement, slow cooling, fast cooling, near-

基金项目: 中国海洋石油集团有限公司"十四·五"科技重大项目(No.KJGG2021-0100);国家科技重大专项(No.2016ZX050266);国家重点基础研究发展计划"973"项目(No.2009CB219400);国家自然科学基金项目(No.91528303);中国海洋石油集团有限公司科技项目(No. 20211-KT-YXKY-05)资助 .

作者简介: 杨海长(1976－),男,高级工程师,从事海洋油气勘探综合地质研究 . ORCID:0009-0009-2421-8198. E-mail:yanghzh1@cnooc. com. cn
* **通讯作者:** 纪沫,ORCID:0000-0002-0772-1893. E-mail:jimo@cnooc. com. cn

引用格式: 杨海长,唐华风,纪沫,田志文,高有峰,2025. 琼东南盆地松南低凸起晚三叠世花岗岩潜山形成和演化 . 地球科学,50(6):2124－2143.

Citation: Yang Haizhang, Tang Huafeng, Ji Mo, Tian Zhiwen, Gao Youfeng, 2025. Formation and Evolution of the Late Triassic Granite Buried Hill in the Songnan Low Uplift, Qiongdongnan Basin. *Earth Science*, 50(6): 2124－2143.

surface denudation and sediments burial.

Key words: Qiongdongnan basin; Songnan low uplift; granite buried hill; petrogenesis; tectonic evolution; petrology; geochronology.

0 引言

琼东南盆地位于华南板块南端、印支地块和太平洋板块交汇部位，中－新生代受古特提斯构造域和古太平构造域影响，经历了复杂的洋壳俯冲、闭合、块体增生与碰撞、洋壳扩张等地质过程（毛建仁等，2014；Zheng *et al.*，2019；吴福元等，2020；李三忠等，2022；徐长贵等，2024）. 近年来随着中国海油的大力勘探开发，琼东南盆地在花岗岩潜山勘探方面取得重大突破（施和生等，2019；张功成等，2023），同时为研究基底花岗岩提供了更多新的资料. 前人对琼东南盆地基底花岗岩进行了一系列研究，研究表明花岗岩形成时代主要为晚二叠世、三叠纪和白垩纪，而在花岗岩岩石成因类型和形成构造背景这些科学问题的认识上还存在争议，如三叠纪花岗岩是古特提斯洋壳俯冲形成、还是板块碰撞－碰撞后伸展形成、还是古太平洋板块俯冲形成（钟佳和王岩泉，2022；Mi *et al.*，2023；胡林等，2024；徐长贵等，2024）. 另外，盆地基底花岗岩潜山中发育岩浆岩脉（周虎等，2024），这些岩脉对于幔源岩浆活动和伸展构造环境具有一定的指示意义. 此外，盆地基底花岗岩锆石(U-Th)/He和磷灰石裂变径迹年代学研究报道较少（Tang *et al.*，2024），缺乏花岗岩潜山剥露成山演化过程研究. 因此，本文对松南低凸起Y8-A井基底花岗岩进行锆石U-Pb年代学、主微量元素、Sr-Nd-Pb-Hf同位素、磷灰石裂变径迹和锆石(U-Th)/He年代学分析，进一步完善松南低凸起花岗岩潜山成岩－成山－埋藏演化过程研究，以期为区域构造演化和盆地花岗岩潜山研究提供新的约束.

1 区域地质背景及样品特征

琼东南盆地是南海北部呈北东走向的新生代陆缘拉张型盆地（张功成等，2010），其北部为海南岛隆起和神狐隆起，南部为西沙隆起，西部为莺歌海盆地，东部为珠江口盆地. 盆地基底可分为前震旦系、震旦系－古生界和中生界基底，其中中生代基底主要为印支期、燕山早期和燕山晚期侵入岩和火山岩（唐历山等，2017）. 新生代南海北部变为伸张环境，盆地经历裂陷、裂后热沉降、加速沉降（解习农等，2011）. 由于断陷期构造及强烈的断裂活动，盆地可划分为12个凹陷和8个低凸起，其中松南低凸起被松南宝岛凹陷、陵水凹陷和北礁凹陷所环绕（图1a）. 松南低凸起花岗岩主要为印支期花岗岩，岩体上覆地层自下而上为渐新统崖城组和陵水组、中新统三亚组、梅山组和黄流组、上新世莺歌海组以及第四系乐东组（图1b）.

本文样品来自松南低凸起Y8-A井，钻遇深度为3 294～3 543 m，主要为二长花岗岩，可见基性岩脉. 肉红色中细粒碎裂二长花岗岩/二长花岗斑岩（图2a）：岩屑呈肉红色，中细粒花岗结构或斑状结构，主要矿物有斜长石、钾长石、石英和黑云母（图2b，2c）；斜长石，自形－半自形为主，大小在0.5～2.0 mm，可见聚片双晶，有高岭土化，碎裂化、绢云母化蚀变；钾长石，半自形板状，大小在1 mm左右，见微斜长石，部分见卡式双晶，有高岭土化蚀变，碎裂化；石英，半自形粒状，大小在1 mm左右，可见波状消光，单偏光镜下矿物表面较干净；黑云母，他形片状，分布在长石颗粒之间，绿泥石化蚀变，含量较少；岩屑还包含二长斑岩岩屑，斑晶为斜长石，碱性长石. 灰黑色蚀变辉绿岩岩脉（图2d）：岩屑呈灰黑色，主要矿物有斜长石、普通辉石（图2e，2f），次要矿物有黑云母，整体碳酸盐化蚀变严重；斜长石，半自形短柱状，大小在0.2～0.5 mm，正低突起，干涉色为一级灰白，有高岭土化、钠黝帘石化蚀变，杂乱分布，似辉绿结构；普通辉石，因蚀变颗粒表面较脏，他形粒状，充填在斜长石粒间，多发生帘石化蚀变；黑云母，褐色、片状，大小在0.2 mm，有绿泥石化.

2 分析方法

花岗岩样品锆石U-Pb定年分析，锆石单矿物分选由在河北省廊坊市区域地质调查研究所完成，通过阴极发光(CL)图像对比分析，选择晶形完好、无裂隙及包裹体、环带清晰锆石颗粒用于U-Pb年龄和Hf同位素测试. LA-ICP-MS锆石U-Pb同位素测定在自然资源部东北亚实验室完成. 锆石U-Pb

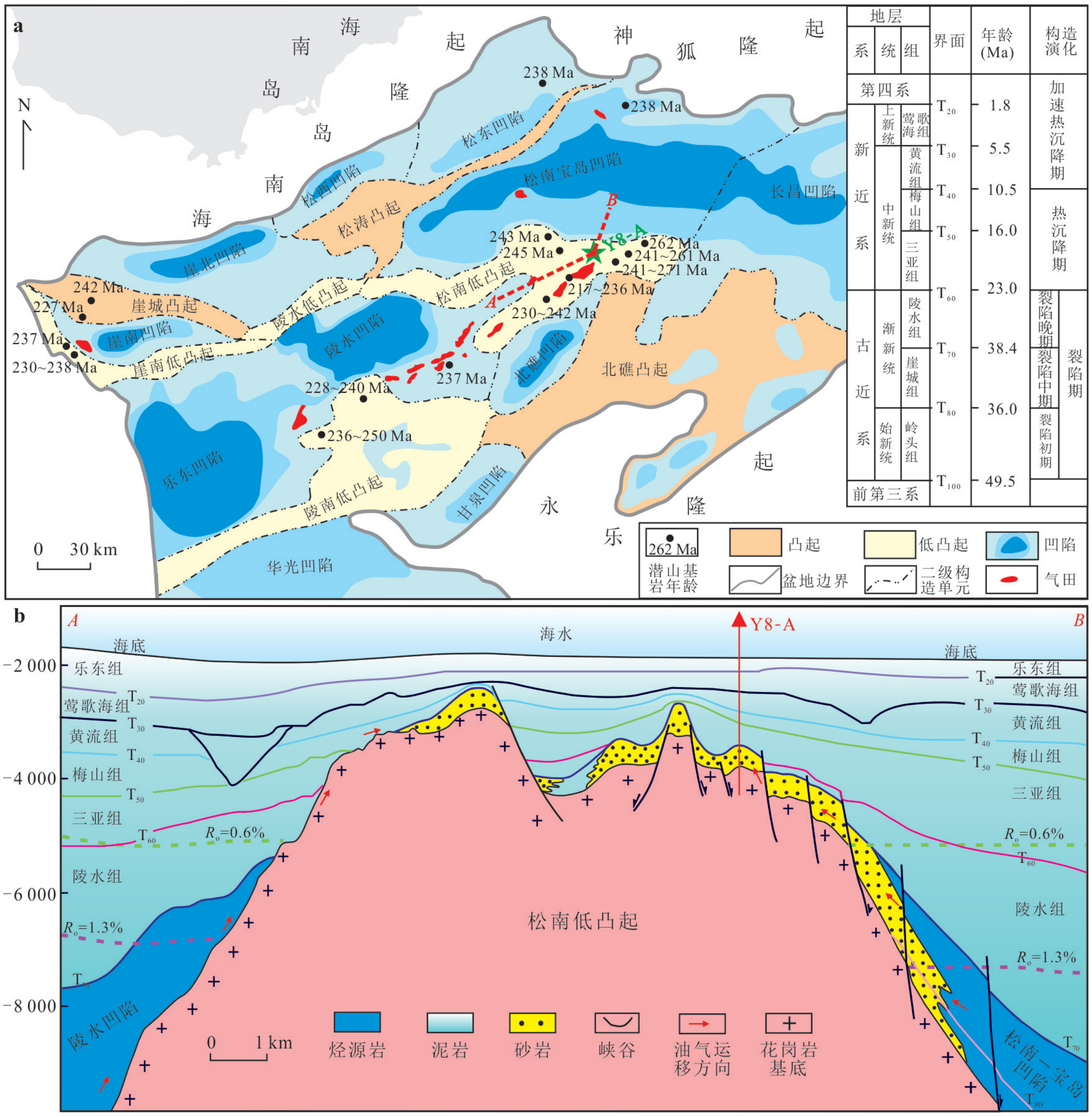

图1 琼东南盆地构造单元(a)及松南低凸起剖面图(b)

Fig.1 Tectonic unit of the Qiongdongnan Basin (a), and profile of the Songnan low uplift (b)

a.据钟佳和王岩泉(2022);b.据杨计海等(2019).潜山基岩年龄数据来源于徐长贵等(2024)

定年测试测试仪器为COMPEx GeoLas Pro型193 nm ArF准分子激光器和Agilent7900型ICP-MS仪器,He作为剥蚀物质的载气,仪器最佳化采用美国国家标准技术研究院研制的人工合成硅酸盐玻璃标准参考物质NIST 610,采用91500标准锆石外部校正法进行锆石原位U-Pb分析,采用32 μm、频率7 Hz的激光束斑.测试数据采用GLITTER软件计算同位素比值和$^{207}Pb/^{206}Pb$、$^{206}Pb/^{238}U$、$^{207}Pb/^{235}U$的年龄值,Andersen(2002)的方法对结果进行普通铅校正,Isoplot4.15宏程序完成协和图、加权平均年龄和年龄频谱图的计算.

花岗岩全岩主微量元素分析,对样品进行挑选、酸处理、清洗、烘干,之后将样品磨碎至200目.主微量元素测试在自然资源部东北亚实验室完成.主量元素化学分析利用日本理学ZSX Primus Ⅱ X射线荧光光谱仪(XRF)分析完成.微量元素和稀土元素分析采用Agilent7500a型电感耦合等离子质谱仪(ICP-MS)测定,误差小于5%.具体方法和参数详见刘晔等(2007)和李文庆(2019).

花岗岩全岩Sr-Nd-Pb同位素分析,对样品进行挑选、酸处理、清洗、烘干、磨碎至200目,元素质量分数和同位素比值分别在Agilent 7700x四级杆型ICP-MS和Nu Plasma Ⅱ 多接收电感耦合等离子质谱仪(MC-ICP-MS)上测定.同位素比值测定选取

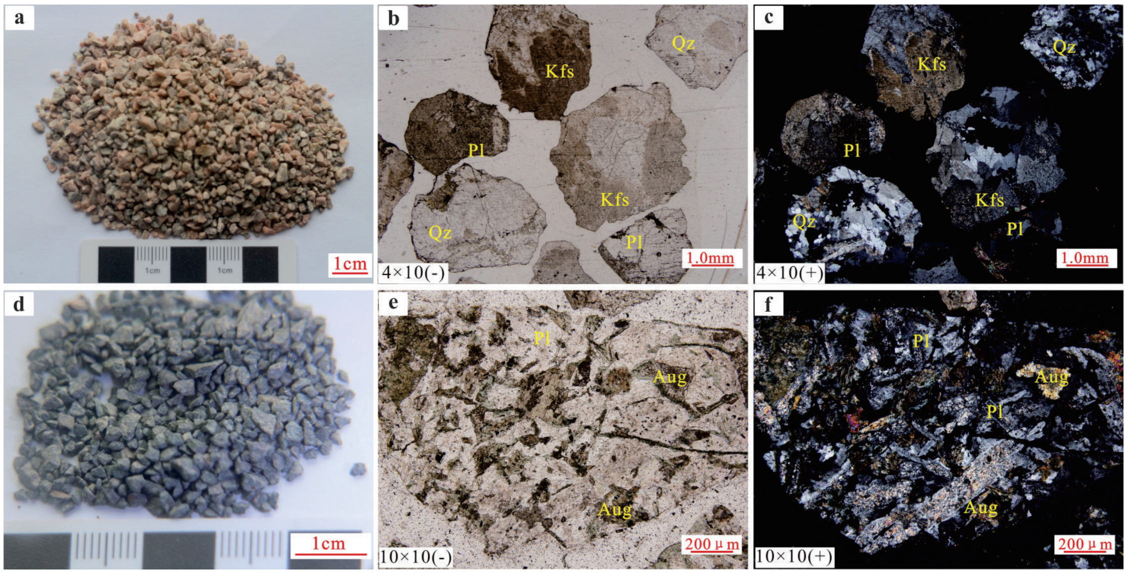

图2 松南低凸起Y8-A井基底花岗岩岩屑、基性岩脉岩屑照片和显微照片

Fig.2 Photos and micrographs of basement granite cuttings and basic dike cuttings of the well Y8-A in the Songnan low uplift

a.肉红色中细粒碎裂二长花岗岩/二长花岗斑岩岩屑；b.二长花岗岩单偏光镜下照片；c.二长花岗岩正交偏光镜下照片；d.灰黑色辉绿岩岩屑；e.蚀变辉绿岩单偏光镜下照片；f.蚀变辉绿岩正交偏光镜下照片；Aug.普通辉石；Kfs.钾长石；Pl.斜长石；Qz.石英

NIST SRM 987、JNdi-1、NIST SRM 981分别作为Sr、Nd、Pb的外表来校正仪器的漂移.具体方法和参数详见郝宇杰等(2020).

锆石Lu-Hf同位素分析，在LA-ICP-MS锆石定年的基础上，根据锆石阴极发光(CL)图像，进行Lu-Hf同位素分析定点，测试仪器为激光剥蚀多接收等离子质谱仪(COMPEx GeoLas Pro型193nm ArF准分子激光器和Neptune Plus)，激光斑束为44 μm，8 Hz，剥蚀时间为26 s，He气作为载气.$\varepsilon_{Hf}(t)$的计算采用^{176}Lu衰常数为$1.867\times10^{-11}\ a^{-1}$，球粒陨石现今的$^{176}Hf/^{177}Hf=0.282\ 785$、$^{176}Lu/^{177}Hf=0.033\ 6$(Blichert-Toft *et al.*，1997).Hf亏损地幔模式年龄(t_{DM1})的计算采用现今的亏损地幔$^{176}Hf/^{177}Hf=0.283\ 25$和$^{176}Lu/^{177}Hf=0.038\ 4$(Griffin *et al.*，2000).两阶段Hf模式年龄(t_{DM2})计算，采用大陆地壳平均的$^{176}Lu/^{177}Hf=0.015$(Griffin *et al.*，2002).

对基性岩脉样品进行破碎，碎至60～80目，镜下挑选除去斑晶.将样品置于5%的稀硝酸中浸泡，用离子水清洗后，低温烘干；将待测样品、标样及用于校正K_2SO_4、CaF_2、KCl按一定次序置于真空石英瓶中，进行中子照射；照射工作在岷江试验堆(MJTR)进行，其*J*值的误差<1‰，分析精度优于2‰，相关参数详见Zhang *et al.* (2023)；质谱分析是在Argus VI-MC型质谱仪上进行，每个峰值均采集20组数据；中子照射过程中所产生的干扰同位素校正系数通过分析照射过的K_2SO_4和CaF_2获得，其$(^{36}Ar/^{37}Ar_0)_{Ca}=0.000\ 369\ 1$，$(^{40}Ar/^{39}Ar)_K=0.028\ 738\ 6$，$(^{39}Ar/^{37}Ar)_{Ca}=0.000\ 860\ 2$.^{37}Ar经过放射性衰变校正，^{40}K衰变常数$\lambda=5.543\times10^{-10}a^{-1}$.采用Ar-Ar CALC Version 2.40进行Ar-Ar年龄计算，得到坪年龄、等时线年龄、反等时线年龄信息.

3 结果

3.1 锆石U-Pb定年

Y8-A井花岗岩锆石共分析30个测试点，其中谐和点有16个，测试数据见附表1和图3.样品锆石晶体呈柱状，自形程度高，长短轴比介于1∶1～1∶2.锆石CL图显示锆石具有明显清晰的振荡环带(图3)，其Th含量为128×10^{-6}～377×10^{-6}，U含量为201×10^{-6}～$1\ 673\times10^{-6}$，Th/U比值介于0.19～0.63，表明锆石为岩浆结晶成因.在U-Pb谐和图中，谐和数据点均落在谐和线或其附近(图4)，表明锆石没有遭受明显的后期构造－热事件影响.16个锆石$^{206}Pb/^{238}U$年龄变化范围介于(221.4±5.2)～(248.8±5.8) Ma，加权平均年龄为235.6±4.8 Ma (MSWD=2.6，*n*=16)，代表了该岩体的结晶年龄，表明Y8-A井花岗岩形成于晚三叠世早期.

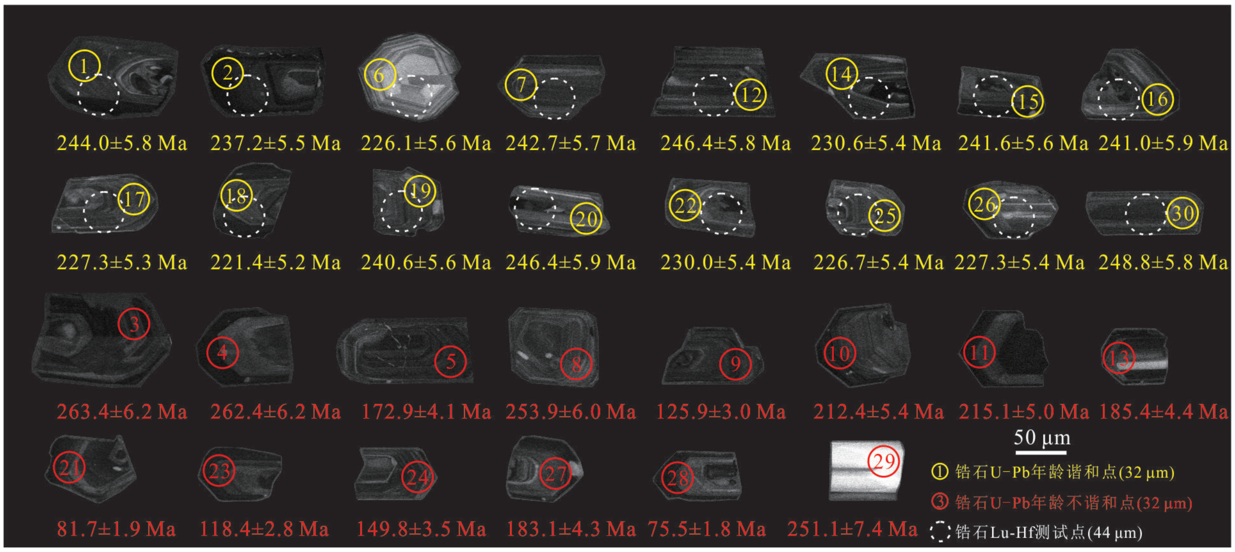

图3　松南低凸起Y8-A井中生代花岗岩锆石CL图

Fig.3　CL images of zircons from the well Y8-A in the Songnan low uplift

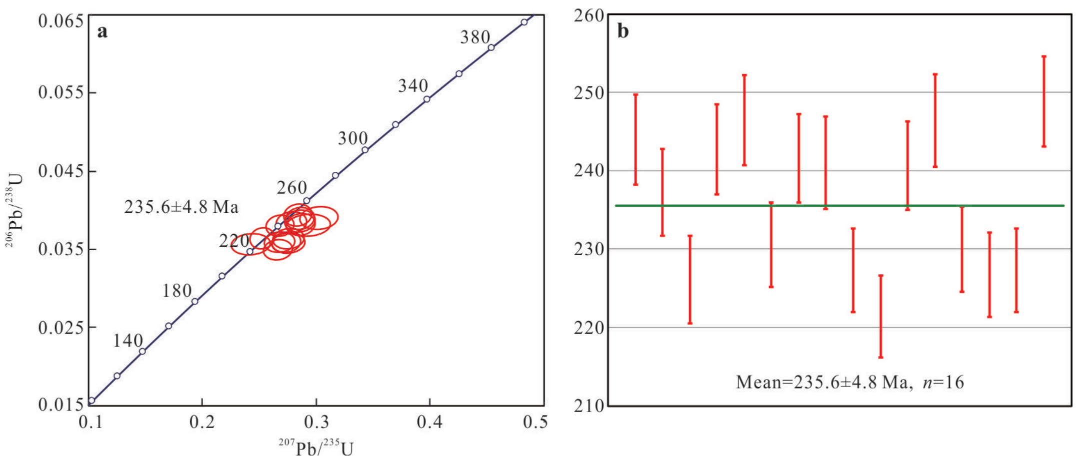

图4　松南低凸起Y8-A井花岗岩锆石U-Pb谐和图(a)和加权平均年龄图(b)

Fig.4　LA-ICP-MS U-Pb concordia diagram (a) and weighted mean age diagram (b) for the zircons from well Y8-A granite in the Songnan low uplift

3.2　主微量元素

Y8-A井6件二长花岗岩样品主量元素分析结果见附表2.SiO_2含量为71.43%～75.78%,Al_2O_3含量为14.07%～16.47%, TiO_2含量为0.15%～0.25%,MgO含量为0.01%～0.09%,CaO含量为0.30%～0.38%,Fe_2O_3含量为0.25%～0.45%,FeO含量为0.13%～0.36%, K_2O含量为4.63%～5.25%,Na_2O含量为3.68%～4.36%,P_2O_5含量为0.01%～0.02%,MnO含量为0.00%～0.01%.烧蚀量介于0.86%～1.09%,表明样品蚀变程度较低.碱质含量K_2O+Na_2O介于8.30%～9.59%,在岩石判别图解上样品分别落入到花岗岩区域(图5a).在SiO_2-K_2O图解上,样品落入高钾钙碱性系列(图5b).铝过饱和指数(A/CNK)介于1.21～1.26,A/NK介于1.27～1.33,样品落入过铝质区域(图5c).SiO_2与Al_2O_3、CaO、K_2O、TiO_2、FeO、MgO、P_2O_5含量呈负相关(图6).

Y8-A井6件花岗岩样品稀土和微量元素分析结果见附表2.样品稀土元素总含量(REE)介于12.34×10^{-6}～28.44×10^{-6},平均值为19.32×10^{-6},$(La/Yb)_N$=1.76～3.22,样品显示弱的Eu正异常(δEu=0.95～1.39).球粒陨石标准化稀土元素配分曲线显示(图7a),样品轻稀土相对富集(LREE/HREE介于2.63～4.62),轻、重稀土分馏明显,显示右倾的稀土配分模式.原始地幔标准化微量元素蛛网图上(图7b),样品显示相对富集Rb、U、K、Pb、

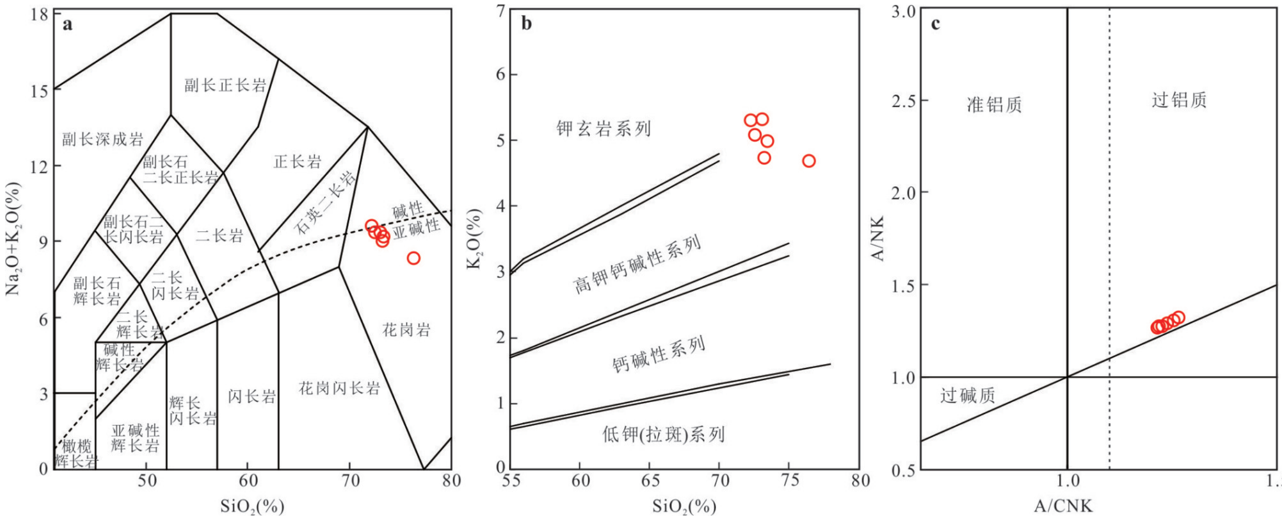

图 5　松南低凸起 Y8-A 井花岗岩 TAS 图解(a)、K_2O-SiO_2 图解(b)和 A/NK-A/CNK 图解(c)

Fig.5　Total alkalis (K_2O+Na_2O) vs. SiO_2 (TAS) (a), K_2O vs. SiO_2 (b), and A/NK (molar ratio $Al_2O_3/(Na_2O+K_2O)$) vs. A/CNK (molar ratio $Al_2O_3/(CaO+Na_2O+K_2O)$) (c) diagrams for the well Y8-A granite in the Songnan low uplift

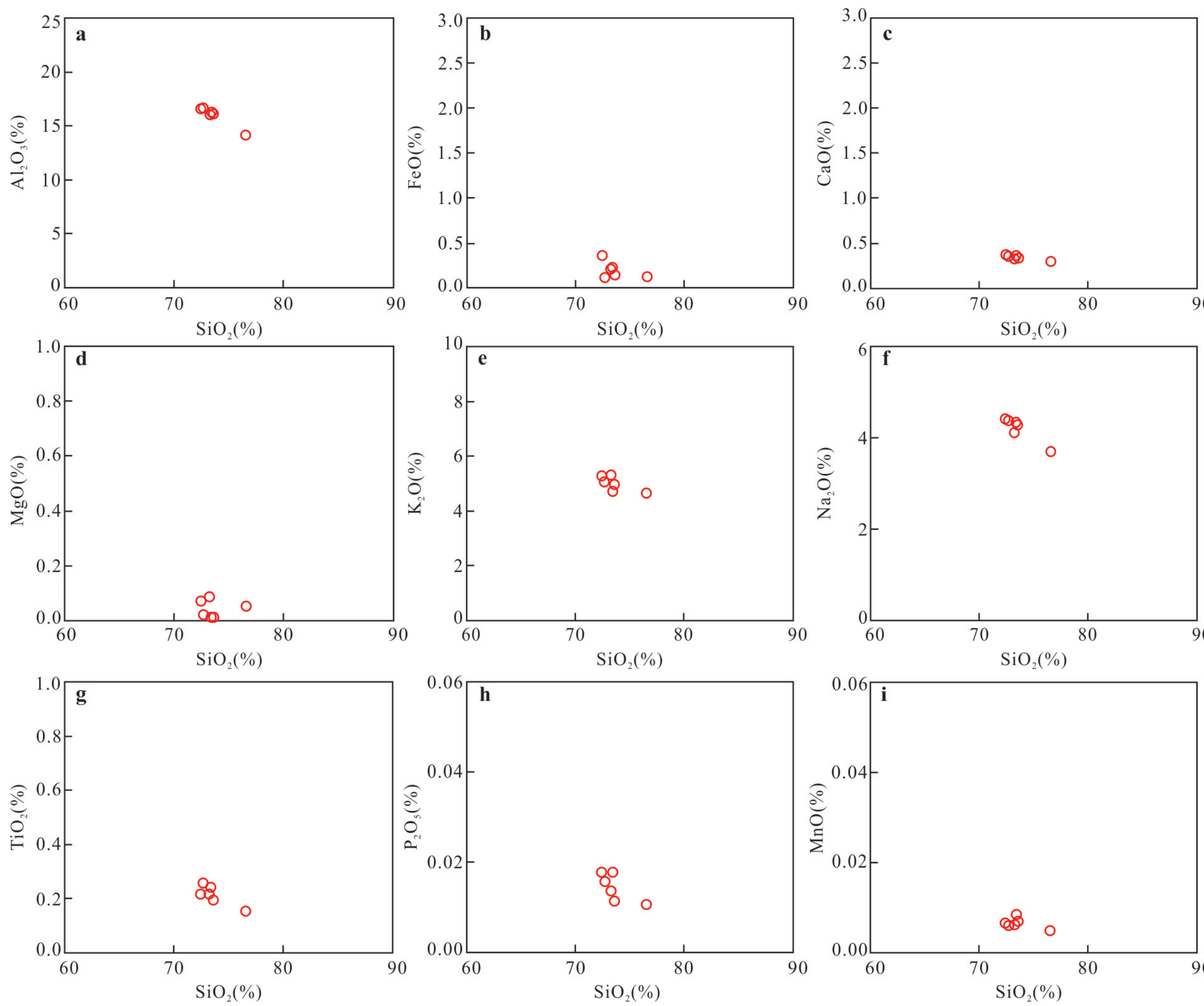

图 6　松南低凸起 Y8-A 井中生代花岗岩哈克图解

Fig.6　Harker diagram of the well Y8-A granite in the Songnan low uplift

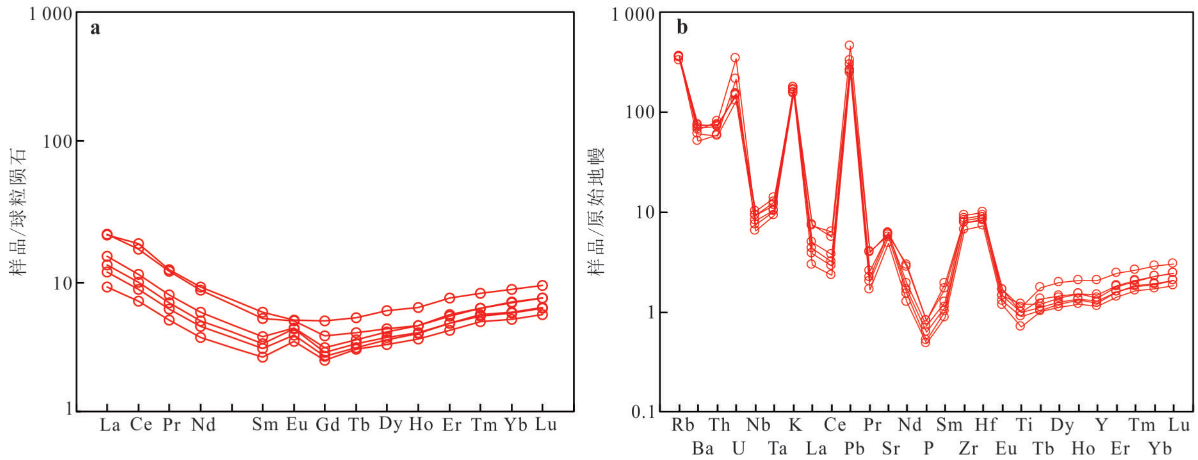

图7 松南低凸起Y8-A井中生代花岗岩球粒陨石标准化稀土元素配分模式图(a)和原始地幔标准化微量元素蛛网图(b)(标准化值据Sun and McDonough,1989)

Fig.7 Chondrite-normalized REE (a) patterns and primitive mantle-normalized trace element spider (b) diagrams for the well Y8-A granite in the Songnan low uplift (the Chondrite and primitive mantle values are from Sun and McDonough,1989)

Sr、Zr、Hf元素,相对亏损Nb、Ta、La、Ce、Pr、P元素.

3.3 Sr-Nd-Pb 同位素

Y8-A井二长花岗岩Sr-Nd-Pb同位素组成见附表3.6件样品的初始Sr、Nd同位素组成用其对应的锆石U-Pb年龄值236 Ma进行校正计算.测得$^{87}Sr/^{86}Sr$比值为0.724 408~0.730 238,平均值为0.726 530.$^{143}Nd/^{144}Nd$比值为0.512 225~0.512 291,平均值为0.512 264.校正计算后初始$(^{87}Sr/^{86}Sr)_i$比值为0.707 93~0.709 44,平均值为0.708 61;初始$(^{143}Nd/^{144}Nd)_i$值为0.512 007~0.512 106,平均值为0.512 061;$\varepsilon_{Nd}(t)$值为-4.45~-6.39,平均值为-5.33;二阶段模式年龄t_{DM2}介于1 373~1 527 Ma,平均值1 442 Ma.在$^{86}Sr/^{87}Sr$-$\varepsilon_{Nd}(t)$图解中,样品落在海南岛二叠纪花岗岩区域,部分落在三叠纪花岗岩区域(图8a,8b).

6件样品测得$^{206}Pb/^{204}Pb$值为18.981~19.356,$^{207}Pb/^{204}Pb$值为15.673~15.695,$^{208}Pb/^{204}Pb$值为38.833~38.930.根据成岩年龄236 Ma计算,$(^{206}Pb/^{204}Pb)_i$值为18.453~18.830,$(^{207}Pb/^{204}Pb)_i$值为15.646~15.664,$(^{208}Pb/^{204}Pb)_i$值为38.631~38.702,μ值为9.90~10.17,$\Delta\beta$值为23.14~24.54,$\Delta\gamma$值为46.67~49.29.样品Pb同位素趋势与海南岛三叠纪花岗岩趋势相似(图8c,8d).

3.4 锆石Lu-Hf同位素

在锆石U-Pb同位素分析的基础上,选取16个点进行锆石Hf同位素分析,分析数据见附表4和图9.测得$^{176}Hf/^{177}Hf$值介于0.282 478~0.282 698,平均值为0.282 555;$^{176}Lu/^{177}Hf$值介于0.000 717~0.010 860,平均值为0.002 330;锆石$\varepsilon_{Hf}(t)$值介于-5.6~1.5,平均值为-2.8;Hf同位素单阶段模式年龄(t_{DM1})介于888~1 096 Ma,二阶段模式年龄(t_{DM2})介于1 162~1 612 Ma.

3.5 $^{40}Ar/^{39}Ar$ 定年

Y8-A基性岩脉样品测试数据详见附表5,样品得到$^{40}Ar/^{39}Ar$坪年龄为141.57±0.63 Ma,正反等时线年龄分别为140.1±1.6 Ma和140.0±1.5 Ma,坪年龄和等时线年龄差距不大(图10).$^{40}Ar/^{36}Ar$初始比值为366±70,略高于大气氩$^{40}Ar/^{36}Ar$初始比值的295.5,说明测试结果有较好的可信度.

4 讨论

4.1 花岗岩岩石成因及岩浆源区

琼东南盆地松南低凸起Y8-A井二长花岗岩LA-ICP-MS锆石U-Pb年龄为235.6±4.8 Ma,形成时代为晚三叠世早期.现今花岗岩根据成因分类通常分为I、S、M、A型(White and Chappell,1983).对于花岗岩成因类型判断,Y8-A井花岗岩为高钾钙碱性、过铝质岩石,高全碱含量(K_2O+Na_2O=8.30%~9.59%).在花岗岩成因类型10 000 Ga/Al-Nb判别图解中(图11a),样品落入到I & S型花岗岩区域,而非A型花岗岩.在Rb-Th和Rb-Y图解中(图11b,11c),样品Rb与Th和Y呈现负相关性,显示出S型花岗岩特征.A/CNK值为1.21~1.26(平

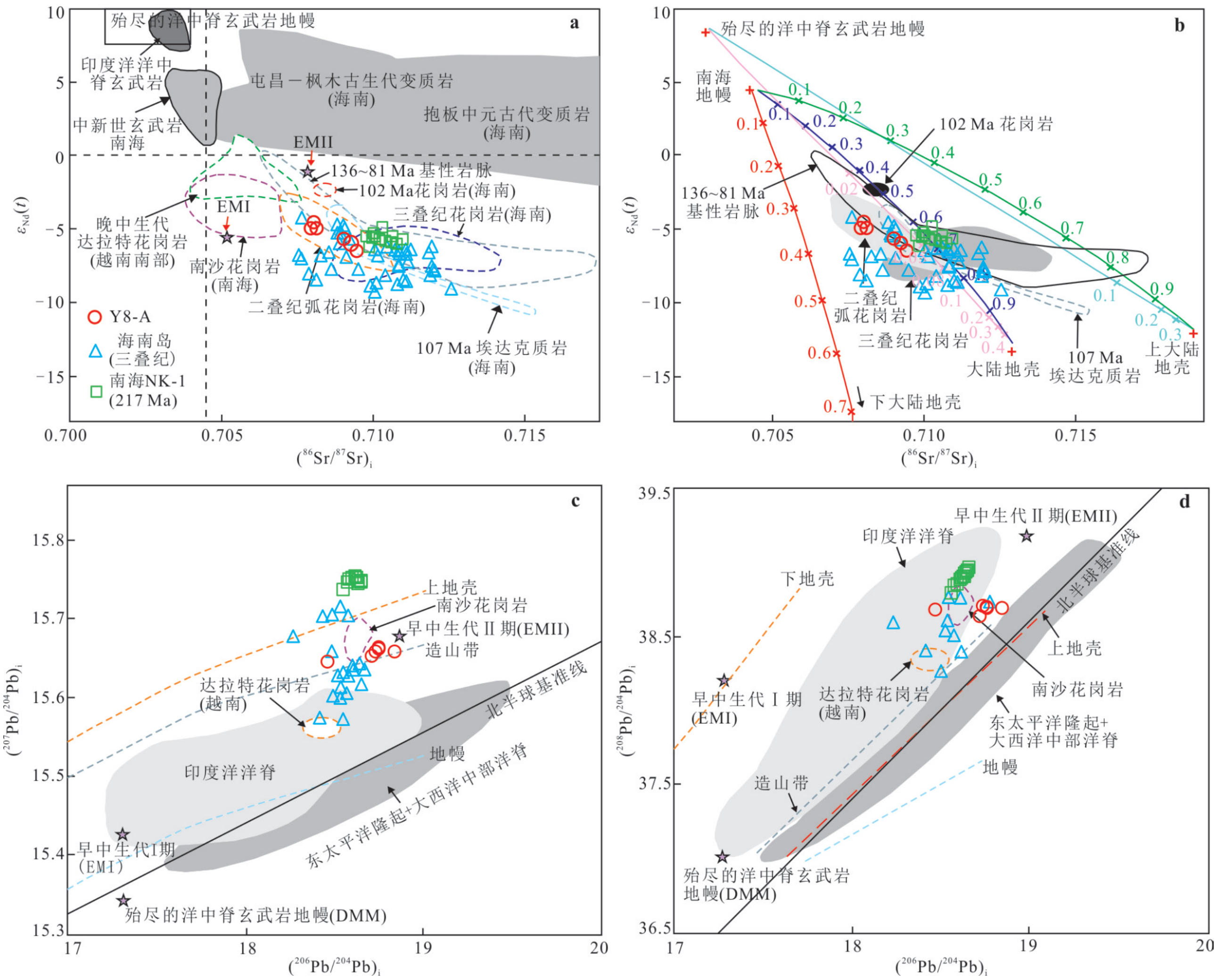

图 8　松南低凸起 Y8-A 井花岗岩判别图解

Fig.8　Diagrams for the well Y8-A granite in the Songnan Low Uplift

a.$\varepsilon_{Nd}(t)$-$(^{86}Sr/^{87}Sr)_i$判别图解;b.$\varepsilon_{Nd}(t)$-$(^{86}Sr/^{87}Sr)_i$判别图解;c.$(^{207}Pb/^{204}Pb)_i$-$(^{2206}Pb/^{204}Pb)_i$判别图解;d. $(^{2208}Pb/^{204}Pb)_i$-$(^{2206}Pb/^{204}Pb)_i$判别图解. a~d.底图及参数详见 Yan *et al.* (2017);海南岛数据来源于葛小月等(2003),余金杰等(2012),Yan *et al.* (2017),苟琪钰等(2019),Cao *et al.* (2022);南海 NK-1 井数据来源于 Miao *et al.* (2021)

均值为 12.3),K_2O/Na_2O 值为 1.08~1.29(平均值为 1.19,其值均大于 1.0;Zhao *et al.*,2015),具有 S 型花岗岩特征.利用锆石饱和温度计估算 Y8-A 井花岗岩结晶温度,其值介于 614~715 ℃(平均值为 653 ℃),低于 A 型花岗岩结晶温度(T_{Zr}>870 ℃).因此,本文认为 Y8-A 井晚三叠世早期二长花岗岩属于 S 型花岗岩.

S 型花岗岩是一种以壳源沉积物为源岩经过部分熔融、结晶而产生的花岗岩.从样品稀土元素组成以及稀土配分模式上看,轻重稀土分馏明显,Eu 呈弱正异常,且重稀土有略微富集的趋势与前人相比不同(钟佳和王岩泉,2022;Mi *et al.*,2023),重稀土略微富集趋势可能为岩浆源区含有石榴子石残留相.样品微量元素显示相对富集 Rb、U、K、Pb、Sr、Zr、Hf 元素,相对亏损 Nb、Ta、La、Ce、P 元素,表现出壳源特征.$^{206}Pb/^{204}Pb$ 值为 18.981~19.356,高于 18.000; $^{207}Pb/^{204}Pb$ 值为 15.673~15.695, 大于 15.300,显示铀铅富集的特征;$^{208}Pb/^{204}Pb$ 值为 38.833~38.930,低于 39.000,显示钍铅微弱亏损;高 μ((9.79~10.17)>9.58)暗示铅同位素基本来源于上地壳,下地壳或上地幔铅可能未参与.在 Zartman and Haines (1988) 的 $^{206}Pb/^{204}Pb$-$^{207}Pb/^{204}Pb$ 和 $^{206}Pb/^{204}Pb$-$^{208}Pb/^{204}Pb$ 图解中(图 12a~12c),样品点落在上地壳区域内.利用 $\Delta\beta$-$\Delta\gamma$ 图解可以示踪铅的源区(朱炳泉,1998)(图 12d),样品点均落在上地壳铅区域.松南低凸起 YL8-A 井二长花岗岩样品 I_{Sr} 值

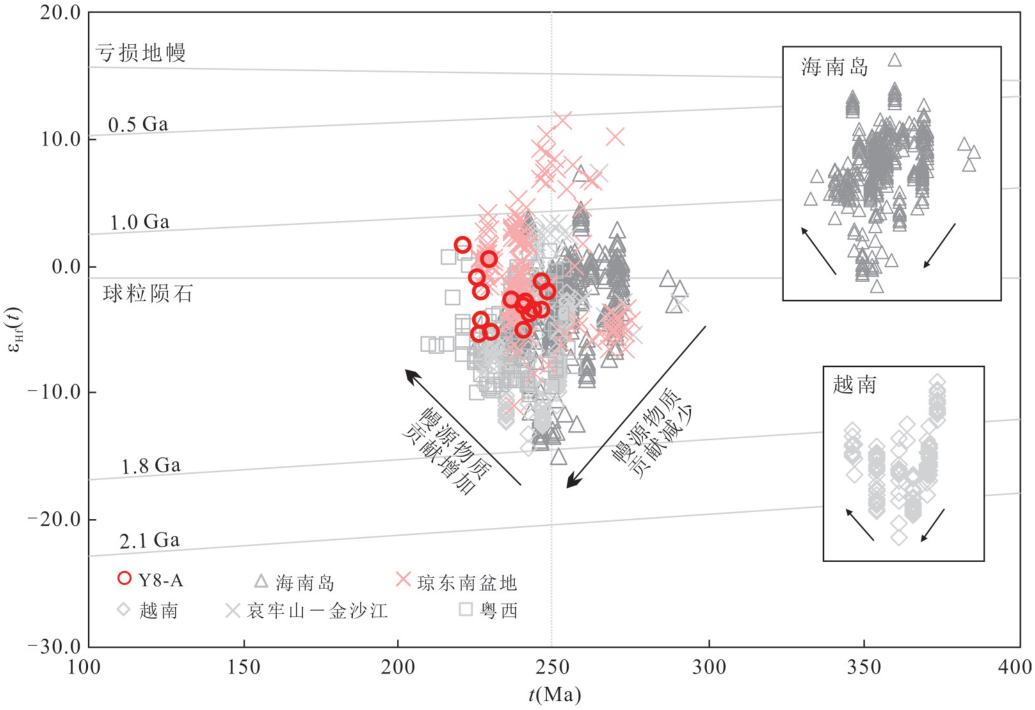

图 9　松南低凸起 Y8-A 基底花岗岩锆石 $\varepsilon_{Hf}(t)$-t 图解

Fig.9　$\varepsilon_{Hf}(t)$-t diagram for the well Y8-A granite in the Songnan low uplift

海南岛数据来源于温淑女等(2013),Shen *et al.* (2018),赵国锋等(2018),Cao *et al.* (2022),吕方等(2023),齐重向等(2023);琼东南盆地数据来源于 Mi *et al.* (2023),徐长贵等(2024),周虎等(2024);越南数据来源于 Chen *et al.*(2014),Thanh *et al.*(2019),李慧玲等(2023);哀牢山－金沙江数据来源于李龚健等(2013),巩小栋等(2020);粤西数据来源于周岱等(2021)

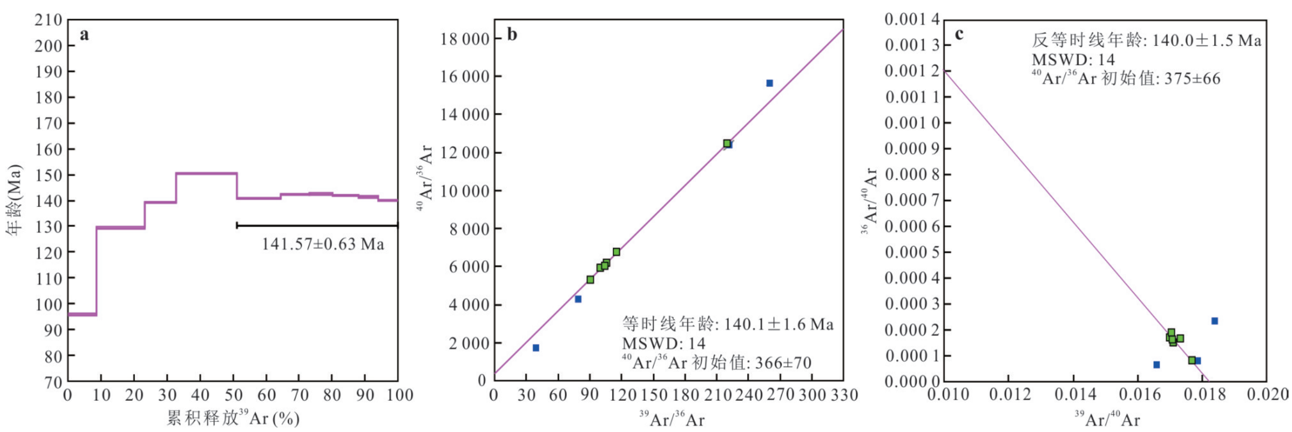

图 10　松南低凸起 Y8-A 井基性岩脉 $^{40}Ar/^{39}Ar$ 年龄谱(a)、等时线(b)和反等时线(c)

Fig.10　Age spectrum (a), isochron (b) and inverse isochron (c) of ^{40}Ar-^{39}Ar basic dike in well Y8-A, Songnan low uplift

(0.707 93～0.709 44)和 $\varepsilon_{Nd}(t)$ 值(－4.45～－6.39),具有高 I_{Sr} 值和低 $\varepsilon_{Nd}(t)$ 值特征.在 $^{86}Sr/^{87}Sr$-$\varepsilon_{Nd}(t)$ 图解中(图 8a,8b),YL8-A 样品落在海南岛二叠纪花岗岩区域,部分落在三叠纪花岗岩区域,岩体的二阶段模式年龄 t_{DM2} 介于 1 373～1 527 Ma,表明中元古代物质对岩浆源区具有明显贡献.锆石 Hf 同位素研究结果表明(图 9),锆石 $\varepsilon_{Hf}(t)$ 值主要为－5.6～－1.1,平均值为－3.4;Hf 同位素二阶段模式年龄(t_{DM2})主要为 1 326～1 612 Ma,平均值为 1 482 Ma,同样暗示岩浆的源区岩石为中元古代地壳物质.另外,在锆石 $\varepsilon_{Hf}(t)$-t 图解中(图 9),海南岛、越南北部、琼东南盆地二叠纪－三叠纪花岗岩锆石 $\varepsilon_{Hf}(t)$ 值在早三叠纪之前呈现出随年龄减小,$\varepsilon_{Hf}(t)$ 值减小趋势(幔源物质贡献减小),而早三叠纪之后随年龄减小,$\varepsilon_{Hf}(t)$ 值增大趋势(幔源贡献物质增大),如海南岛尖峰岭早三叠世花岗岩为后造山环境岩石圈拆

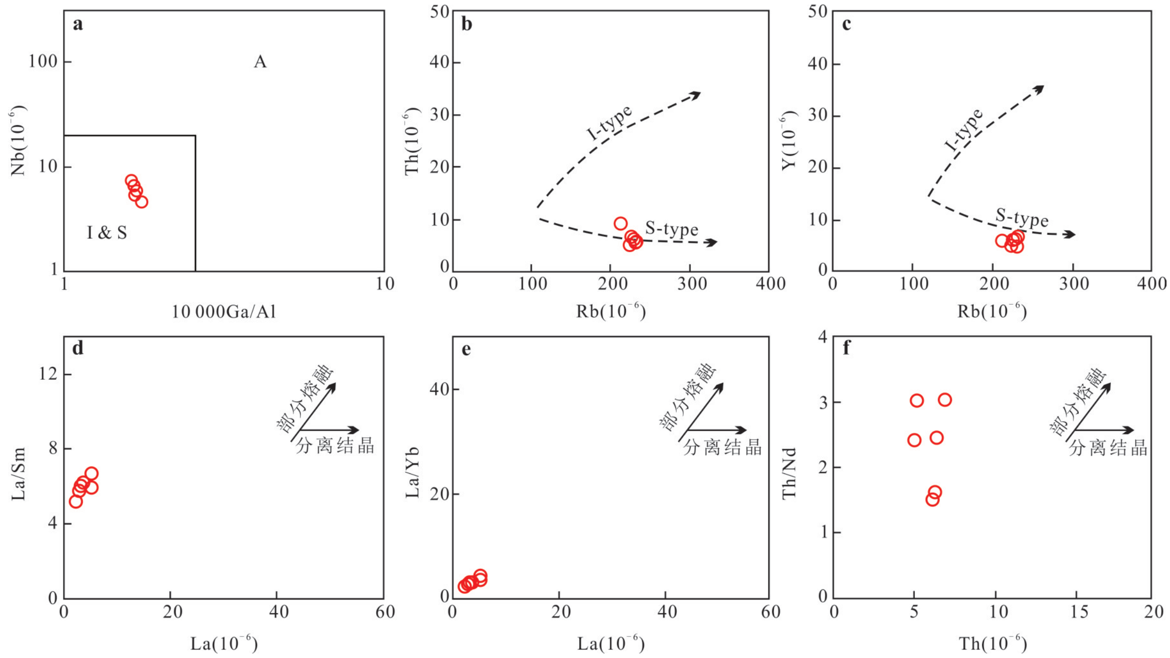

图 11　松南低凸起 Y8-A 井花岗岩 Nb-10 000 Ga/Al (a)、Th-Rb (b)、Y-Rb (c)、La/Sm-La (d)、La/Yb-La (e)、Th/Nd-Th (f)判别图解

Fig.11　Nb-10 000 Ga/Al (a), Th-Rb (b), Y-Rb (c), La/Sm-La (d), La/Yb-La (e), Th/Nd-Th (f) discrimination diagrams for the well Y8-A granite in the Songnan low uplift

沉、热软流圈上涌,使得地壳变杂砂岩或变砂屑岩受到幔源流体富集后发生部分熔融(谢才富等,2006);海南岛通什地区中三叠世正长花岗岩由石英正长岩结晶分异形成,而石英正长质岩浆可能是来源于EM2的碱性玄武质岩浆在地壳再分异派生的产物(周佐民等,2011);南海南部NK-1井晚三叠世英安岩为中下陆壳古玄武岩物质部分熔融产物(Miao *et al.*,2021).

在部分熔融和分离结晶的La-La/Sm、La-La/Y、Th-Th/Nd图解中(图11d~11f),松南低凸起二长花岗岩表现出部分熔融趋势.Harker图解中(图6),SiO_2与Al_2O_3、CaO、K_2O和Sr含量呈负相关,表明钾长石和斜长石可能经历一定程度的分离结晶;与TiO_2、FeO、MgO呈负相关表明黑云母和Fe-Ti氧化物可能发生分离结晶;与P_2O_5含量呈负相关,表明磷灰石可能发生一定程度结晶分离.花岗岩CaO/Na_2O值介于0.08~0.09(CaO/Na_2O<0.3为泥质岩重熔,>0.3为砂质岩重熔),表明其是变泥质岩部分熔融的产物.基于岩石地球化学及Sr-Nd-Pb-Hf同位素研究,松南低凸起晚三叠世早期二长花岗岩属于高钾钙碱性、过铝质系列的S型花岗岩,初始岩浆主要来源于上地壳变泥质岩的部分熔融.

4.2　大地构造意义

目前南海北部和海南岛三叠纪花岗岩是由古特提斯洋俯冲形成(Yan *et al.*,2017;徐长贵等,2024;胡林等,2024),还是古太平洋俯冲形成(刘飞等,2022;Mi *et al.*,2023);它们形成于挤压碰撞的构造环境,还是处于后造山的构造环境(谢才富等,2005),这些科学问题的认识仍存在争议.因此对于这些问题首先要了解古特提斯洋和古太平洋在南海北部地区构造演化.首先是对于古特提斯洋在南海北部地区的俯冲闭合演化.古特提斯不同洋盆俯冲闭合时限具有差异性,同一洋盆不同地段闭合时限也不同.巩小栋等(2020)认为金沙江结合带晚三叠世石英二长岩形成于金沙江古特提斯洋逐渐闭合后碰撞环境.Fan *et al.* (2010) 对澜沧江南带岩浆作用研究认为古特提斯洋盆的俯冲闭合在250~225 Ma.李龚健等(2013)认为哀牢山缝合带闭合时限在晚二叠世(~260 Ma),金沙江古特提洋闭合时限为早三叠世(~245 Ma),昌宁—孟连地区古特提洋闭合时限为中三叠世(~235 Ma).Wang *et al.* (2018) 认为中—晚三叠世时期金沙江—哀牢山—松马构造带已处于同碰撞—后碰撞的构造背景.Zhang *et al.* (2014) 在松马构造带中发现230 Ma古特提斯洋俯冲闭合印支和华南板块碰撞形成的榴

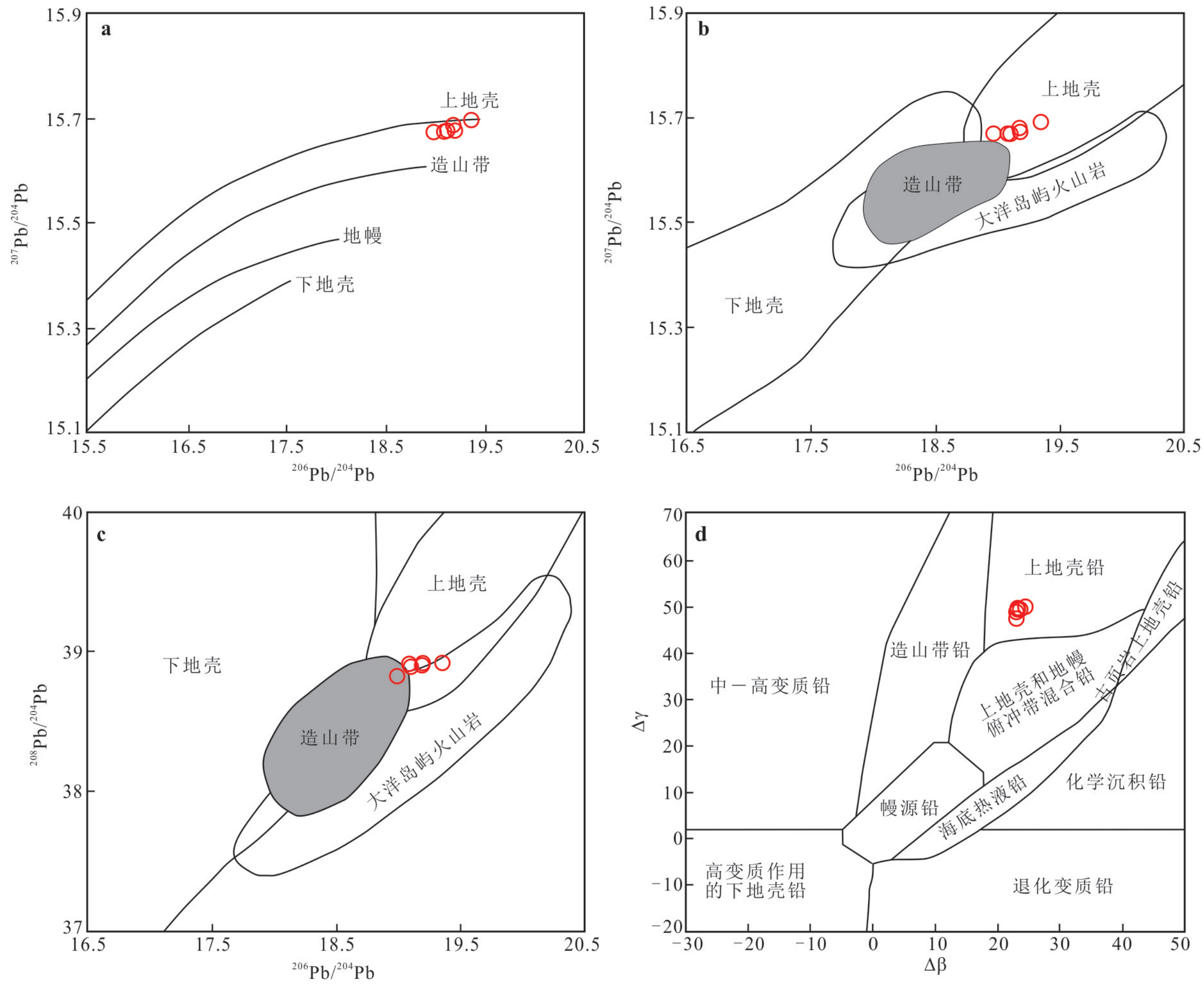

图 12 松南低凸起 Y8-A 基底花岗岩 $^{207}Pb/^{204}Pb$-$^{206}Pb/^{204}Pb$(a,b)、$^{208}Pb/^{204}Pb$-$^{206}Pb/^{204}Pb$(c)、$\Delta\gamma$-$\Delta\beta$(d)图解

Fig.12 $^{207}Pb/^{204}Pb$-$^{206}Pb/^{204}Pb$ (a, b), $^{208}Pb/^{204}Pb$-$^{206}Pb/^{204}Pb$ (c), and $\Delta\gamma$-$\Delta\beta$ (d) discrimination diagrams for the well Y8-A granite in the Songnan Low Uplift

辉岩.李慧玲等(2023)认为越南昆嵩地体中三叠世花岗岩形成于后碰撞阶段,与马江古特提斯分支洋闭合后印支与华南陆块碰撞拼合有关.罗伟等(2023)认为川西晚三叠世花岗细晶岩形成于松潘—甘孜洋(古特提斯支洋)闭合后的碰撞造山阶段.唐立梅等(2013)认为海南岛东南部兴隆地区238~234 Ma双峰式侵入岩的形成与古特提斯俯冲闭合有关.苟琪钰等(2019)认为海南岛南部三亚荔枝沟地区中三叠世酸性火山岩形成于碰撞闭合后的伸展环境.Yan *et al.* (2017) 对海南岛二叠、三叠和白垩纪花岗岩研究认为海南岛晚二叠世—中三叠世受古特提斯俯冲影响.Li *et al.*(2016)对广西钦州中二叠世S型花岗岩分析提出古特提洋东部俯冲始于中二叠世,闭合于中三叠世.周岱等(2021)提出粤西晚三叠世新兴花岗岩可能形成于古特提斯洋东段闭合后陆陆碰撞造山阶段.钟佳和王岩泉(2022)认为琼东南盆地松南低凸起花岗岩形成于华南与印支地块后碰撞阶段.徐长贵等(2024)和胡林等(2024)提出琼东南盆地早三叠世花岗岩形成与古特提斯俯冲汇聚和同碰撞有关,晚三叠世花岗岩形成于碰撞后伸展背景.综上,古特提斯洋在南海北部地区俯冲闭合可能在中三叠世之前完成.基于前人对金沙江—哀牢山—松马构造带、越南地区、海南岛、广西、广东、琼东南盆地地区古特提斯相关研究,认为南海北部地区晚二叠世—早三叠世为古特提斯洋俯冲闭合阶段(图 13a),中三叠世为印支—华南地块碰撞阶段(图 13b),晚三叠世为碰撞后伸展阶段.

另外,S型花岗岩岩体通常是大洋闭合和陆—陆碰撞使地壳加厚并发生部分熔融的产物(Pearce *et al.*,1984).在 Y-Nb、Y+Nb-Rb 和 Rb/30-Hf-3×Ta 图解上(图 14a~11c),花岗岩样品落入火山弧花

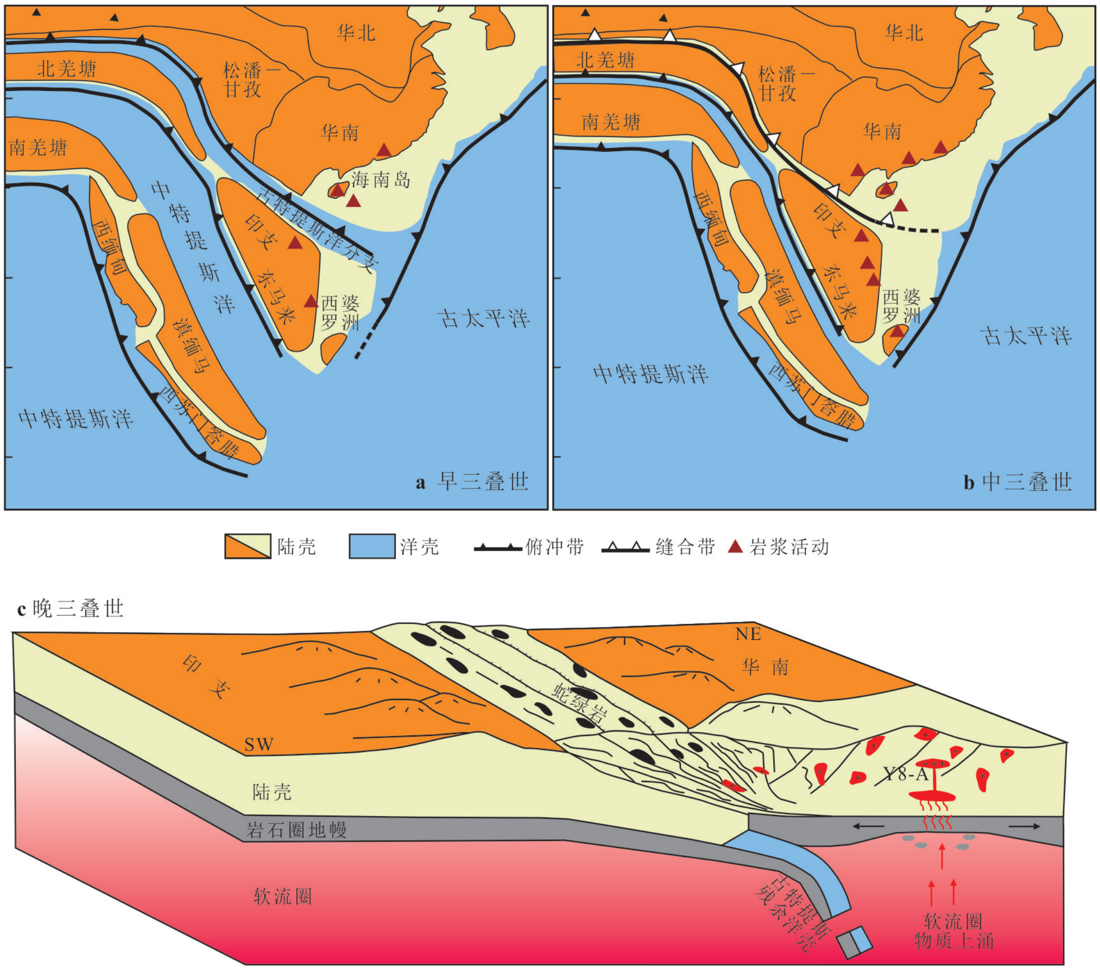

图 13　早三叠世(a)和中三叠世(b)南海及邻区板块构造演化重建及 Y8-A 井花岗岩岩浆成因示意图(c)

Fig.13　Early Triassic (a) and Middle Triassic (b) reconstruction of plate tectonic evolution in the South China Sea and adjacent areas, and well Y8-A granite magma genesis schematic diagram(c)

据 Hennig *et al.* (2017); Zheng *et al.* (2019); Tian *et al.* (2021)

岗岩和同碰撞花岗岩交界区域.在 R_1-R_2图解上(图 14d),样品落在同碰撞花岗岩区域附近.这表明松南低凸起晚三叠世花岗岩可能是碰撞或后碰撞相关的岩浆作用.松南低凸起二长花岗岩形成年龄为晚三叠世早期,而晚三叠世琼东南盆地地区处于后碰撞阶段,加厚地壳发生拆沉,软流圈物质上涌,导致区域的伸展作用,使得变沉积岩发生部分熔融形成花岗岩(图 13c).

一些学者认为海南岛和琼东南盆地晚二叠纪—三叠纪花岗岩的形成与古太平洋俯冲有关.刘飞等(2022)提出金波晚二叠世二长花岗岩和早三叠世辉绿岩形成于大陆岛弧挤压向伸展过渡的构造环境,为古太平洋板片向欧亚板块俯冲后撤的产物.Mi *et al.* (2023) 认为琼东南盆地晚二叠世—白垩纪花岗岩具有火山弧特征,与古太平洋板块俯冲有关.但是,目前多数学者认为古特提斯构造域向古太平洋构造域转换时间在早侏罗世(毛建仁等,2014;李三忠等,2022).Wang and Shu(2012)对福建侏罗—白垩纪火成岩研究认为早侏罗世晚期以后华南东部经历了从特提斯域向古太平洋域的构造过渡.Xu *et al.*(2019)对广东永安盆地和粤东盆地沉积岩碎屑锆石年龄进行分析,提出早侏罗世是特提斯构造域向古太平洋构造域转变的时间.Tan *et al.* (2024)对中国东南部中生代构造应力场及福建地区沉积地层研究,认为华南东部早三叠世—中侏罗世早期的构造演化主要受古特提斯构造域控制,而中侏罗世晚期—白垩世的构造演化主要受古太平洋构造域控制.海南岛和琼东南盆地地区三叠纪花岗岩的形成受古特提斯构造域控制的观点依然是目前的主流观点.

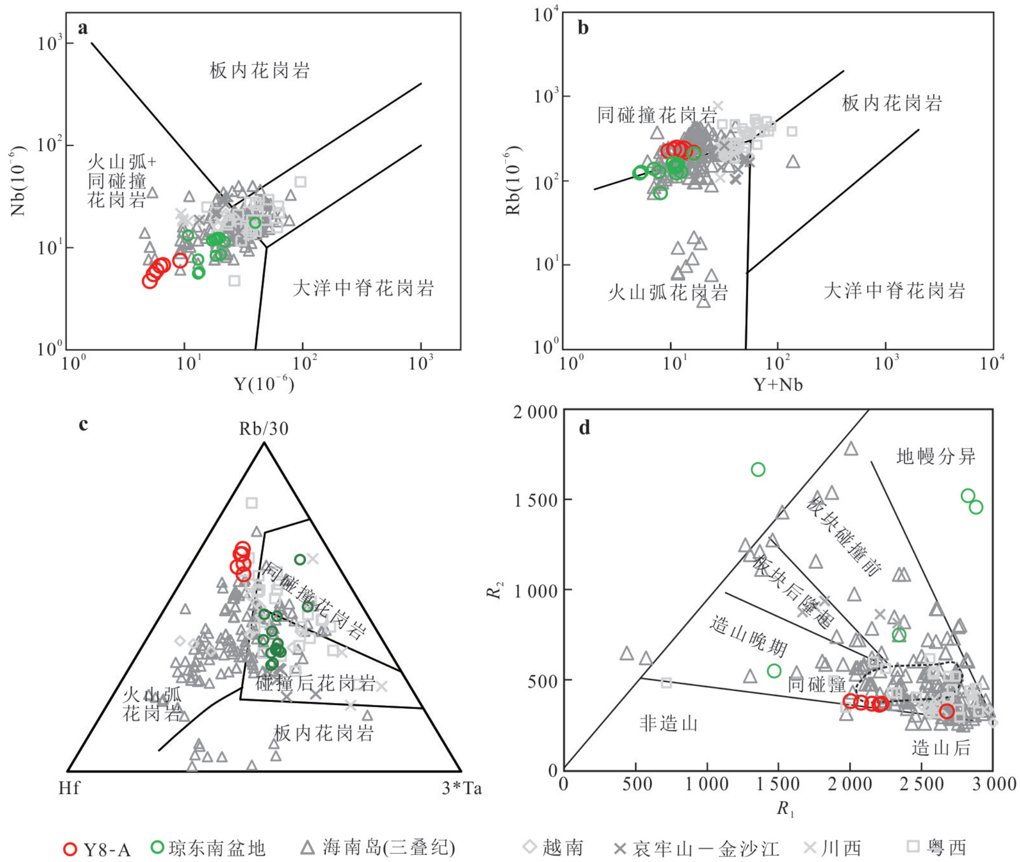

图 14　松南低凸起 Y8-A 井基底花岗岩 Nb-Y(a)、Rb-Y＋Nb(b)、Rb/30-Hf-3×Ta(c)和 R_2-R_1(d)判别图解

Fig.14　Nb-Y (a), Rb-Y＋Nb (b), Rb/30-Hf-3×Ta (c) and R_2-R_1 (d) diagrams for the well Y8-A granite in the Songnan low uplift

R_1=4Si－11(Na＋K)－2(Fe＋Ti)，R_2=6Ca＋2Mg. 海南岛数据来源于葛小月(2003)，谢才富等(2006)，余金杰等(2012)，Yan *et al.* (2017)，Shen *et al.* (2018)，赵国锋等(2018)，苟琪钰等(2019)，吕昭英等(2019)，Cao *et al.* (2022)，吕方等(2023)，齐重向等(2023)；琼东南盆地数据来源于钟佳和王岩泉(2022)，Mi *et al.* (2023)，徐长贵等(2024)；越南数据来源于Chen *et al.*(2014)，李慧玲等(2023)，Thanh *et al.* (2019)；哀牢山－金沙江数据来源于李龚健等(2013)，巩小栋等(2020)；川西数据来源于罗伟等(2023)；粤西数据来源于周岱等(2021)

4.3　花岗岩岩体热演化史与构造事件

花岗岩岩浆侵位和冷凝后，在内外动力作用下相对于地表运移，并逐渐出露地表. 利用锆石 U-Pb 法、^{40}Ar/^{39}Ar 法、锆石(U-Th)/He、磷灰石裂变径迹法年龄结合上覆沉积地层数据，以不同测年矿物的封闭温度为依据，对岩体热史演化进行模拟(王瑜，2004). 锆石 U-Pb 测年法封闭温度 850～700 ℃，一般被认为是岩浆侵位年龄；全岩 ^{40}Ar/^{39}Ar 测年法封闭温度 300～400 ℃，用来定年和揭露地质体冷却和抬升速率；锆石(U-Th)/He 测年法封闭温度 200～160 ℃，可以用来揭露距地表 7～5 km 深度地质体的冷却年龄和剥露速率；磷灰石裂变径迹测年法封闭温度 120～60 ℃，可以用来揭露距地表 4～2 km 深度地质体的冷却年龄和剥露速率. 这一系列的热年代学数据，分别表示近似岩浆侵位年龄(锆石 U-Pb 年龄)、后期改造年龄(岩脉 ^{40}Ar/^{39}Ar 年龄)、岩体一定深度年龄(锆石(U-Th)/He 年龄)、近地表暴露年龄(磷灰石裂变年龄). 松南低凸起晚三叠世早期二长花岗岩磷灰石裂变径迹年龄为(66.3±5.6) Ma(附表 6)，锆石(U-Th)/He 年龄(82.05±1.99) Ma～(45.93±1.14) Ma，排除异常颗粒，认为锆石(U-Th)/He 年龄为(82.05±1.99) Ma(附表 6). 通过 HeFTy 软件进行热史模拟(图 15)，花岗岩热史演化可以分为 5 个阶段：阶段Ⅰ为侵位冷凝阶段，花岗岩岩浆侵位到地壳一定深度经过一段时间岩浆冷凝；阶段Ⅱ为缓慢冷却阶段，岩浆冷凝后在地壳中一定深度受到构造运动抬升，在地壳一定深度受到构造运动影响而发生抬升，期间在早白垩世伴有基性岩脉侵入；阶段Ⅲ为快速冷却阶段，受到构造作用或上覆地层强烈剥蚀快速向地表运移，上覆地层剥蚀

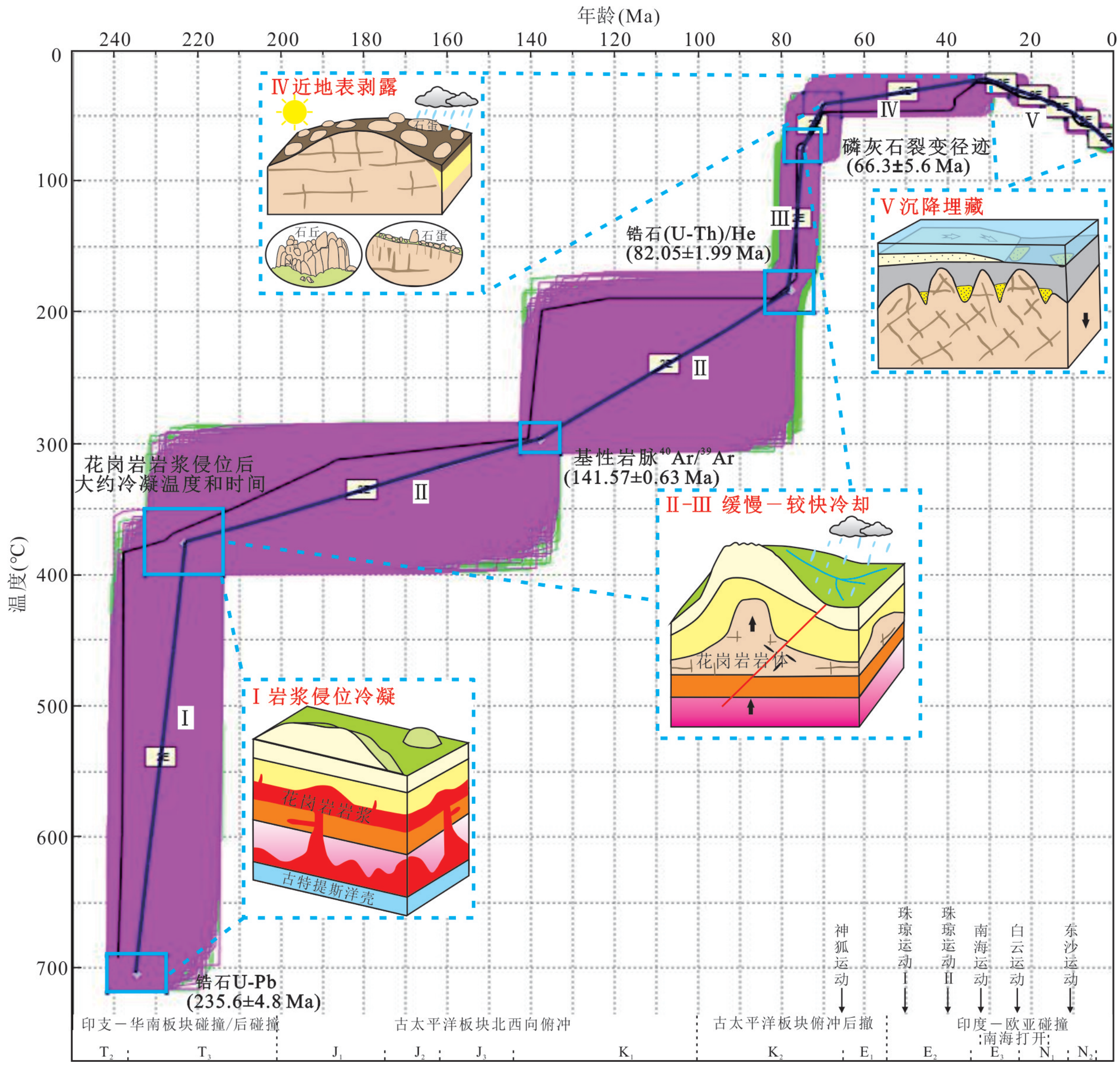

图 15　松南低凸起 Y8-A 井花岗岩热史演化模拟和潜山形成过程

Fig.15　Thermal history evolution simulation and the buried hill formation of granite in the well Y8-A of the Songnan low uplift

速率较快;阶段Ⅳ为近地表阶段,岩体出露地表接受风化剥蚀,花岗岩剥蚀速率相较之前变慢;阶段Ⅴ为埋藏阶段,盆地沉降岩体被沉积物再次覆盖,上覆地层为渐新统黄流组、中新统三亚组、梅山组、黄流组、莺歌海组以及第四纪乐东组.

南海北部中生代经历了印支期碰撞造山、燕山早期增生造山、燕山晚期压扭造山(李三忠等,2022).花岗岩 LA-ICP-MS 锆石 U-Pb 年龄为 235.6±4.8 Ma,表明岩浆侵位时间约在晚三叠世早期,构造背景分析认为岩浆侵位是由古特提斯分支洋壳俯冲所导致,由于印支－华南板块碰撞使得南海北部地壳岩石发生强烈褶皱及韧性剪切变形(高维等,2022;吕方等,2023),岩浆沿断裂上侵冷凝(对应阶段Ⅰ).早三叠世后古特提斯洋盆基本关闭,古太平洋俯冲开始启动(约 200 Ma)(李三忠等,2022).古太平洋的强烈俯冲表现在中国东南沿海地区广泛发育侏罗－白垩纪 NE 向分布的侵入岩(毛建仁等,2014),南海北部变为挤压环境,产生一系列 NE 向左行走滑断裂(熊莉娟等,2012;鲁宝亮等,2015),南海北部及周缘发生增生和压扭造山(对应阶段Ⅱ).另外板块之间相互作用使得位置发生调整,导致板块内部形成伸展环境,基性岩脉上侵.在海南、广东、福建以及南海北部盆地花岗岩中可见到基性岩脉(陈新跃等,2014;刘飞等,2022).胡瑞忠等(2007)认为华南地区可能存在 6 期伸展构造,最早一期为 145～135 Ma,而 YL8-A 中基性岩脉年龄

与其相对应.此外,曹建劲等(2009)提出广东沿海地区基性岩脉年龄介于146～54 Ma,并将其划分为5期,其中第一期为146 Ma.晚白垩世,西太平洋俯冲带发生后撤,南海北部地区由挤压环境逐步向伸展环境转变,岩石圈大规模伸展减薄,始新世可能为拉张减薄高峰阶段,如在广东沿海发育有基性岩脉(54 Ma)和珠江口盆地发育有侵入岩和火山岩(43 Ma)(祝嵩等,2021;周凤娟等,2023).另外,构造体制的转换使得华南南部地区中生界地层抬升,使得上覆盖层被强烈剥蚀(Suo *et al.*,2019),造成相对较快的隆升(对应阶段Ⅲ).南海北部地区新生代以来经历古南海俯冲消亡、南海洋盆扩张、印度欧亚板块碰撞、菲律宾海板块北西西向运动、海南地幔柱以及红河断裂左旋走滑(雷超等,2015),琼东南盆地受神狐运动、珠琼运动、南海运动、白云运动、东沙运动等影响,经历断陷阶段和拗陷阶段(吴克强等,2023).古新世—始新世,松南低凸起晚三叠世早期的花岗岩岩体可能已出露地表或在近地表(对应阶段Ⅳ),另外花岗岩岩体剥蚀速率相较于沉积地层较慢.始新世—至今琼东南盆地总体表现为沉降特征(杨军等,2015)(对应阶段Ⅴ),岩体上覆缺失渐新统陵水组地层,表明松南低凸起可能受到南海运动或白云运动的影响.

5 结论

琼东南盆地松南低凸起Y8-A井二长花岗岩LA-ICP-MS锆石U-Pb年龄为235.6±4.8 Ma,基性岩脉^{40}Ar-^{39}Ar坪年龄为141.57±0.63 Ma.二长花岗岩属于高钾钙碱性、过铝质系列的S型花岗岩,初始岩浆主要来源于上地壳变泥质岩的部分熔融.结合前人研究和区域地质背景分析认为花岗岩形成于印支与华南碰撞拼和后的后碰撞背景.

对松南低凸起二长花岗岩进行低温热年代学分析,结果显示磷灰石裂变径迹年龄为66.3±5.6 Ma,锆石(U-Th)/He年龄为(82.05±1.99)～(45.93±1.14) Ma.联合热史反演结果揭示,花岗岩岩体的演化可分为侵位冷凝、缓慢冷却、较快冷却、近地表剥露和沉降埋藏5个阶段.

附表见地球科学官网:https://doi.org/10.3799/dqkx.2025.051

References

Andersen, T., 2002. Correction of Common Lead in U-Pb Analyses that Do Not Report ^{204}Pb. *Chemical Geology*, 192(1-2): 59-79. https://doi.org/10.1016/s0009-2541(02)00195-x

Blichert-Toft, J., Chauvel, C., Albarède, F., 1997. Separation of Hf and Lu for High-Precision Isotope Analysis of Rock Samples by Magnetic Sector-Multiple Collector ICP-MS. *Contributions to Mineralogy and Petrology*, 127(3): 248-260. https://doi.org/10.1007/s004100050278

Cao, G.Y., Li, X., Xie, G.G., et al., 2022. Petrogenesis of Late Permian to Middle Triassic Magmatic Rocks on Northern Hainan Island, South China: Implications for Crust-Mantle Interaction and the Tectonic Evolution of the Paleo-Tethys. *Journal of Asian Earth Sciences*, 234:105238. https://doi.org/10.1016/j.jseaes.2022.105238

Cao, J.J., Hu, R.Z., Xie, G.Q., et al., 2009. Geochemistry and Genesis of Mafic Dikes from the Coastal Areas of Guangdong Province, China. *Acta Petrologica Sinica*, 25(4):984-1000 (in Chinese with English abstract).

Chen, X.Y., Wang, Y.J., Han, H.P., et al., 2014. Geochemical and Geochronological Characteristics of Triassic Basic Dikes in SW Hainan Island and Its Tectonic Implications. *Journal of Jilin University* (*Earth Science Edition*), 44(3):835-847 (in Chinese with English abstract).

Chen, Z.C., Lin, W., Faure, M., et al., 2014. Geochronology and Isotope Analysis of the Late Paleozoic to Mesozoic Granitoids from Northeastern Vietnam and Implications for the Evolution of the South China Block. *Journal of Asian Earth Sciences*, 86: 131-150. https://doi.org/10.1016/j.jseaes.2013.07.039

Fan, W.M., Wang, Y.J., Zhang, A.M., et al., 2010. Permian Arc-Back-Arc Basin Development along the Ailaoshan Tectonic Zone: Geochemical, Isotopic and Geochronological Evidence from the Mojiang Volcanic Rocks, Southwest China. *Lithos*, 119(3-4):553-568. https://doi.org/10.1016/j.lithos.2010.08.010

Gao, W., Shi, J.R., Meng, Q.K., et al., 2022. Discovery and Geological Significance of the Indosinian Granulites in Hainan Island: New Evidence from U-Pb Dating and Trace Element Composition of Zircons. *Acta Geologica Sinica*, 96(2): 426-444(in Chinese with English abstract).

Ge, X.Y., 2003. Mesozoic Magmatism in Hainan Island (SE China) and Its Tectonic Significance: Geochronology, Geochemistry and Sr-Nd Isotope Evidences (Dissertation). Guangzhou Institute of Geochemistry, Chinese Academy of Sciences, Guangzhou(in Chinese with English abstract).

Gong, X.D., Tang, Y., Qin, Y.D., et al., 2020. Late Triassic Collision of Jinshajiang Suture Belt: Geochronological, Geochemical and Hf Isotope Evidences from Quartz Monzonite in Gonjo Area. *Earth Science*, 45(8): 2905—2919 (in Chinese with English abstract).

Gou, Q.Y., Qian, X., He, H.Y., et al., 2019. Geochronological and Geochemical Constraints on Lizhigou Middle Triassic Felsic Volcanic Rocks in Hainan and Its Tectonic Implications. *Earth Science*, 44(4): 1357—1370 (in Chinese with English abstract).

Griffin, W.L., Pearson, N.J., Belousova, E., et al., 2000. The Hf Isotope Composition of Cratonic Mantle: LAM-MC-ICPMS Analysis of Zircon Megacrysts in Kimberlites. *Geochimica et Cosmochimica Acta*, 64(1): 133—147. https://doi.org/10.1016/s0016-7037(99)00343-9

Griffin, W.L., Wang, X., Jackson, S.E., et al., 2002. Zircon Chemistry and Magma Mixing, SE China: In-Situ Analysis of Hf Isotopes, Tonglu and Pingtan Igneous Complexes. *Lithos*, 61(3—4): 237—269. https://doi.org/10.1016/s0024-4937(02)00082-8

Hao, Y.J., Ren, Y.S., Shi, Y.F., et al., 2020. Geochronology, Petrogenesis and Tectonic Setting of the Granite Porphyry Related to Hekoulinchang Tin Polymetallic Deposit in Wandashan Area, Heilongjiang Province. *Acta Petrologica Sinica*, 36(3): 837—855(in Chinese with English abstract).

Hennig, J., Breitfeld, H.T., Hall, R., et al., 2017. The Mesozoic Tectono-Magmatic Evolution at the Paleo-Pacific Subduction Zone in West Borneo. *Gondwana Research*, 48(1): 292—310. https://doi.org/10.1016/j.gr.2017.05.001

Hu, L., Xiong, F.H., Chen, A.Q., et al., 2024. Granitic Magmatism and Tectonic Evolution in Qiongdongnan Basin and Their Constraints on the Properties of Buried Hill Reservoirs. *Geological Bulletin of China*, 43(7): 1191—1206(in Chinese with English abstract).

Hu, R.Z., Bi, X.W., Peng, J.T., et al., 2007. Some Problems Concerning Relationship between Mesozoic-Cenozoic Lithospheric Extension and Uranium Metallogenesis in South China. *Mineral Deposits*, 26(2): 139—152 (in Chinese with English abstract).

Lei, C., Ren, J.Y., Zhang, J., 2015. Tectonic Province Divisions in the South China Sea: Implications for Basin Geodynamics. *Earth Science*, 40(4): 744—762 (in Chinese with English abstract).

Li, G.J., Wang, Q.F., Yu, L., et al., 2013. Closure Time of the Ailaoshan Paleo-Tethys Ocean: Constraints from the Zircon U-Pb Dating and Geochemistry of the Late Permian Granitoids. *Acta Petrologica Sinica*, 29(11): 3883—3900 (in Chinese with English abstract).

Li, H.L., Qian, X., Yu, X.Q., et al., 2023. Petrogenesis of Triassic Granites from Kontum Massif in Vietnam and Its Tethyan Tectonic Implications. *Earth Science*, 48(4): 1441—1460(in Chinese with English abstract).

Li, S.Z., Suo, Y.H., Zhou, J., et al., 2022. Tectonic Evolution of the South China Ocean-Continent Connection Zone: Transition and Mechanism of the Tethyan to the Pacific Tectonic Domains. *Journal of Geomechanics*, 28(5): 683—704(in Chinese with English abstract).

Li, W.Q., 2019. Testing Accuracy of 10 Major Elements in Diabase by Borate Melting Sample Preparation Method. *Global Geology*, 38(3): 843—851 (in Chinese with English abstract).

Li, Y.J., Wei, J.H., Santosh, M., et al., 2016. Geochronology and Petrogenesis of Middle Permian S-Type Granitoid in Southeastern Guangxi Province, South China: Implications for Closure of the Eastern Paleo-Tethys. *Tectonophysics*, 682: 1—16. https://doi.org/10.1016/j.tecto.2016.05.048

Liu, F., Yang, J.S., Feng, G.Y., et al., 2022. Late Permian to Early Triassic Subduction and Retreating of the Paleopacific slab: Constraints from Continental Arc Magmatism in Hainan Island. *Acta Petrologica Sinica*, 38(11): 3455—3483(in Chinese with English abstract).

Liu, Y., Liu, X.M., Hu, Z.C., et al., 2007. Evaluation of Accuracy and Long-Term Stability of Determination of 37 Trace Elements in Geological Samples by ICP-MS. *Acta Petrologica Sinica*, 23(5): 1203—1210 (in Chinese with English abstract).

Lu, B.L., Wang, P.J., Zhang, G.C., et al., 2015. Characteristic of Regional Fractures in South China Sea and Its Basement Tectonic Framework. *Progress in Geophysics*, 30(4): 1544—1553 (in Chinese with English abstract).

Luo, W., Peng, J., Jin, T.F., et al., 2023. Petrogenesis of Granite Aplite in the Lijiagou Lithium Polymetallic Ore District in Western Sichuan: constraints from Geochemistry, Zircon U-Pb Geochronology and Hf Isotope. *Sedimentary Geology and Tethyan Geology*, 43(1): 36—47 (in Chinese with English abstract).

Lyu, F., Xin, Y.J., Li, J.H., et al., 2023. Permian-Triassic Tectonic Evolution of Hainan Island: Constraints from Geochronology and Geochemistry of Magmatic and Metamorphic Rocks. *Acta Geologica Sinica*, 97(1): 30—51(in Chinese with English abstract).

Lyu, Z.Y., Chen, M.L., Fu, Y.R., et al., 2019. Petrogenesis Study of Two Stages A-Type Granite and Its Geological Significance in Danzhou Area of Hainan Province. *Miner-*

al Resources and Geology, 33(4): 660—669(in Chinese with English abstract).

Mao, J.R., Li, Z.L., Ye, H.M., 2014. Mesozoic Tectono-Magmatic Activities in South China: Retrospect and Prospect. *Science China : Earth Sciences*, 57(12): 2593—2617(in Chinese).

Mi, L.J., Tang, X.Y., Yang, H.Z., et al., 2023. Zircon U-Pb Geochronology, Hf Isotopes, and Geochemistry Constraints on the Age and Tectonic Affinity of the Basement Granitoids from the Qiongdongnan Basin, Northern South China Sea. *Acta Oceanologica Sinica*, 42(3): 19—30. https://doi.org/10.1007/s13131-022-2078-1

Miao, X.Q., Huang, X.L., Yan, W., et al., 2021. Late Triassic Dacites from Well NK-1 in the Nansha Block: Constraints on the Mesozoic Tectonic Evolution of the Southern South China Sea Margin. *Lithos*, 398: 106337. https://doi.org/10.1016/j.lithos.2021.106337

Pearce, J.A., Harris, N.B.W., Tindle, A.G., 1984. Trace Element Discrimination Diagrams for the Tectonic Interpretation of Granitic Rocks. *Journal of Petrology*, 25(4): 956—983. https://doi.org/10.1093/petrology/25.4.956

Qi, Z.X., Wen, S.N., Pang, C.J., et al., 2023. Formation of Middle-Triassic A-Type Granites in Northern Hainan Island and Its Geological Implications. *Geochimica*, 52(1): 69—83(in Chinese with English abstract).

Shen, L.W., Yu, J.H., O'Reilly, S.Y., et al., 2018. Subduction-Related Middle Permian to Early Triassic Magmatism in Central Hainan Island, South China. *Lithos*, 318: 158—175. https://doi.org/10.1016/j.lithos.2018.08.009

Shi, H.S., Yang, J.H., Zhang, Y.Z., et al., 2019. Geological Understanding Innovation and Major Breakthrough to Natural Gas Exploration in Deep Water in Qiongdongnan Basin. *China Petroleum Exploration*, 24(6): 691—698 (in Chinese with English abstract).

Sun, S.S., McDonough, W.F., 1989. Chemical and Isotopic Systematics of Oceanic Basalts: Implications for Mantle Composition and Processes. *Geological Society of London Special Publications*, 42(1): 313—345. https://doi.org/10.1144/GSL.SP.1989.042.01.19

Suo, Y.H., Li, S.Z., Jin, C., et al., 2019. Eastward Tectonic Migration and Transition of the Jurassic-Cretaceous Andean-Type Continental Margin along Southeast China. *Earth-Science Reviews*, 196: 102884. https://doi.org/10.1016/j.earscirev.2019.102884

Tan, Y.L., Wang, Z.X., Li, C.L., et al., 2024. Mesozoic Tectonic Regime Transformation in Fujian Province (Southeast China): Evidence from Palaeostress Field Restoration and Lithofacies Palaeogeography Evolution. *Geological Journal*, 59(2): 701—731. https://doi.org/10.1002/gj.4888

Tang, L.M., Chen, H.L, Dong, C.W., et al., 2013. Middle Triassic Post-Orogenic Extension on Hainan Island: Chronology and Geochemistry Constraints of Bimodal Intrusive Rocks. Science China: *Earth Sciences*, 43(3): 433—445 (in Chinese with English abstract).

Tang, L.S., Zhu, J.T., Yao, Z., et al., 2017. Evolution and Reservoir Formation Conditions of Buried Hills in Songnan Low Uplift of the Qiongdongnan Basin. *Special Oil & Gas Reservoirs*, 24(1): 87—91(in Chinese with English abstract).

Tang, X.Y., Zhang, K.X., Yang, S.C., et al., 2024. Thermal and Exhumation History of the Songnan Low Uplift, Qiongdongnan Basin: Constraints from the Apatite Fission-Track and Zircon (U-Th)/He Thermochronology. *Acta Oceanologica Sinica*, 43(4): 40—49. https://doi.org/10.1007/s13131-023-2253-z

Thanh, T.V., Hieu, P.T., Minh, P., et al., 2019. Late Permian-Triassic Granitic Rocks of Vietnam: The Muong Lat Example. *International Geology Review*, 61(15): 1823—1841. https://doi.org/10.1080/00206814.2018.1561335

Tian, Z.W., Tang, W., Wang, P.J., et al., 2021. Tectonic Evolution and Key Geological Issues of the Proto-South China Sea. *Acta Geologica Sinica (English Edition)*, 95(1): 77—90. https://doi.org/10.1111/1755-6724.14644

Wang, D.Z., Shu, L.S., 2012. Late Mesozoic Basin and Range Tectonics and Related Magmatism in Southeast China. *Geoscience Frontiers*, 3(2): 109—124. https://doi.org/10.1016/j.gsf.2011.11.007

Wang, Y., 2004. Some Thoughts on Tectono-Thermochronology. *Earth Science Frontiers*, 11(4): 435—443(in Chinese with English abstract).

Wang, Y.J., Qian, X., Cawood, P.A., et al., 2018. Closure of the East Paleotethyan Ocean and Amalgamation of the Eastern Cimmerian and Southeast Asia Continental Fragments. *Earth-Science Reviews*, 186: 195—230. https://doi.org/10.1016/j.earscirev.2017.09.013

Wen, S.N., Liang, X.Q., Fan, W.M., et al., 2013. Zircon U-Pb Ages, Hf Isotopic Composition of Zhizhong Granitic Intrusion in Ledong Area of Hainan Island and Their Tectonic Implications. *Geotectonica et Metallogenia*, 37(2): 294—307(in Chinese with English abstract).

White, A.J.R., Chappell, B.W., 1983. Granitoid Types and Their Distribution in the Lachlan Fold Belt, Southeastern Australia. In: Roddick, J.A., ed., Circum-Pacific Plutonic Terranes. Geological Society of America, U.S.A., 21—34. https://doi.org/10.1130/mem159-p21

Wu, F.Y., Wan, B., Zhao, L., et al., 2020. Tethyan Geodynamics. *Acta Petrologica Sinica*, 36(6): 1627－1674(in Chinese with English abstract).

Wu, K.Q., Xie, X.N., Pei, J.X., et al., 2023. Deep Architecture of Hyperextended Marginal Basin and Implications for Hydrocarbon exploration: A Case Study of Qiongdongnan Basin. *Oil & Gas Geology*, 44(3): 651－661(in Chinese with English abstract).

Xie, C.F., Zhu, J.C., Ding, S.J., et al., 2006. Age and Petrogenesis of the Jianfengling Granite and Its Relationship to Metallogenesis of the Baolun Gold Deposit, Hainan Island. *Acta Petrologica Sinica*, 22(10): 2493－2508 (in Chinese with English abstract).

Xie, C.F., Zhu, J.C., Zhao, Z.J., et al., 2005. Zircon SHRIMP U-Pb Age Dating of Garnet-Acmite Syenite: Constraints on the Hercynian-Indosinian Tectonic Evolution of Hainan Island. *Geological Journal of China Universities*, 11(1): 47－57 (in Chinese with English abstract).

Xie, X.N., Zhang, C., Ren, J.Y., et al., 2011. Effects of Distinct Tectonic Evolutions on Hydrocarbon Accumulation in Northern and Southern Continental Marginal Basins of South China Sea. *Chinese Journal of Geophysics*, 54(12): 3280－3291(in Chinese with English abstract).

Xiong, L.J., Li, S.Z., Suo, Y.H., et al., 2012. Cenozoic Basin-Controlling Faults and Their Bearing on Basin Groups Formaion in the Southern South China Sea. *Marine Geology & Quaternary Geology*, 32(6): 113－127 (in Chinese with English abstract).

Xu, C.G., Hou, M.C., Wu, K.Q., et al., 2024. Permian-Triassic Felsic Magmatism in the Qiongdongnan Basin: Implications for the Tectonic Properties and Evolution of the Northern Continental Margin of the South China Sea. *Acta Petrologica Sinica*, 40(8): 2450－2468(in Chinese with English abstract).

Xu, Q.J., Liu, S.F., Wang, Z.F., et al., 2019. Provenance of the East Guangdong Basin and Yong'an Basin in Southeast China: Response to the Mesozoic Tectonic Regime Transformation. *Journal of Asian Earth Sciences*, 185: 104024. https://doi.org/10.1016/j.jseaes.2019.104024

Yan, Q.S., Metcalfe, I., Shi, X.F., 2017. U-Pb Isotope Geochronology and Geochemistry of Granites from Hainan Island (Northern South China Sea Margin): Constraints on Late Paleozoic-Mesozoic Tectonic Evolution. *Gondwana Research*, 49: 333－349. https://doi.org/10.1016/j.gr.2017.06.007

Yang, J., Shi, X.B., Wang, Z.F., et al., 2015. Origin of Syn-Rift Subsidence Deficit and Rapid Post-Rift Subsidence in Qiongdongnan Basin. *Marine Geology & Quaternary Geology*, 35(1): 81－90 (in Chinese with English abstract).

Yang, J.H., Huang, B.J., Yang, J.H., 2019. Gas Accumulation Conditions and Exploration Potentials of Natural Gases in Songnan Low Uplift, Deep Water Area of Qiongdongnan Basin. *China Offshore Oil and Gas*, 31(2): 1－10(in Chinese with English abstract).

Yu, J.J., Chen, F.X., Wang, Y.H., et al., 2012. Origin and Rock-Forming Environment of the Granitoids in the Periphery of the Shilu Iron Deposit. *Geology in China*, 39(6): 1700－1711 (in Chinese with English abstract).

Zartman, R.E., Haines, S.M., 1988. The Plumbotectonic Model for Pb Isotopic Systematics among Major Terrestrial Reservoirs: A Case for Bi-Directional Transport. *Geochimica et Cosmochimica Acta*, 52(6): 1327－1339. https://doi.org/10.1016/0016-7037(88)90204-9

Zhang, G.C., Mi, L.J., Wu, J.F., et al., 2010. Rises and Their Plunges: Favorable Exploration Directions for Major Fields in the Deepwater Area, Qiongdongnan Basin. *China Offshore Oil and Gas*, 22(6): 360－368 (in Chinese with English abstract).

Zhang, G.C., Yang, D.S., Guo, S., et al., 2023. The Formation of Oil and Gas in Basement Buried Hills with Its Model of Three-Element Controlling Reservoir and the Frontiers of Deep Water Oil and Gas Exploration in the Northern South China Sea. *Natural Gas Geoscience*, 34(12): 2045－2061(in Chinese with English abstract).

Zhang, R.Y., Lo, C.H., Li, X.H., et al., 2014. U-Pb Dating and Tectonic Implication of Ophiolite and Metabasite from the Song Ma Suture Zone, Northern Vietnam. *American Journal of Science*, 314(2): 649－678. https://doi.org/10.2475/02.2014.07

Zhang, W.F., Li, J.J., Zheng, D.W., et al., 2023. Sample Neutron Irradiation with the Min Jiang Testing Reactor (MJTR): implications for High-Precision $^{40}Ar/^{39}Ar$ Dating. *Journal of Analytical Atomic Spectrometry*, 38(8): 1540－1548. https://doi.org/10.1039/d3ja00048f

Zhao, G.F., Liu, H.C., Qian, X., et al., 2018. Petrogenesis of Late Permian Ⅰ-Type Granites in SE Hainan Island and Its Tectonic Implication for Paleotethyan Evolution. *Earth Science*, 43(4): 1321－1332 (in Chinese with English abstract).

Zhao, Z.F., Gao, P., Zheng, Y.F., 2015. The Source of Mesozoic Granitoids in South China: Integrated Geochemical Constraints from the Taoshan Batholith in the Nanling Range. *Chemical Geology*, 395: 11－26. https://doi.org/10.1016/j.chemgeo.2014.11.028

Zheng, H., Sun, X.M., Wang, P.J., et al., 2019. Mesozoic Tectonic Evolution of the Proto-South China Sea:A Perspective from Radiolarian Paleobiogeography. *Journal of Asian Earth Sciences*, 179: 37−55. https://doi. org/10.1016/j.jseaes.2019.04.009

Zhong, J., Wang, Y. Q., 2022. Geochronology, Geochemical Characteristics and Tectonic Environment of Granite in Songnan Low Uplift, Qiongdongnan Basin. *Journal of Jilin University* (*Earth Science Edition*), 52(1):134−148 (in Chinese with English abstract).

Zhou, D., Hu, J., Yang, W.Q., et al., 2021. Formation Age and Petrogenesis of the Xinxing Pluton in Western Guangdong: Constraint on the Closure of the East Paleo-Tethys Ocean. *Geology in China*, 48(6): 1896−1923 (in Chinese with English abstract).

Zhou, F.J., Ding, L., Li, X.Y., et al., 2023. Provenance Tracing of Zircon Dating from Wenchang Formation in Zhu Ⅰ Depression and Its Influence on Reservoir. *Unconventional Oil & Gas*, 10(3): 46−54(in Chinese with English abstract).

Zhou, H., Fu, Y.Z., Hu, Q.W., et al., 2024. Geochronology, Geochemistry and Tectonic Setting of Late Triassic Diabase in Buried Hills of Qiongdongnan Basin. *Journal of Chengdu University of Technology* (*Science & Technology Edition*), 51(4):543−560(in Chinese with English abstract).

Zhou, Z.M., Xie, C.F., Xu, Q., et al., 2011. Geological and Geochemical Characteristics of Middle Triassic Syenite—Granite Suite in Hainan Island and Its Geotectonic Implications. *Geological Review*, 57(4): 515−531(in Chinese with English abstract).

Zhu, B.Q., 1998. Study on Chemical Heterogeneities of Mantle Crustal Systems and Geochemical Boundaries of Blocks. *Earth Science Frontiers*, 5(1): 72−82(in Chinese with English abstract).

Zhu, S., Yao, Y.J., Li, X.J., 2021. Spatio-Temporal Distribution Pattern of Magmatic Rocks and Mechanism in the South China Sea and Adjacent Areas. *Marine Geology & Quaternary Geology*, 41(4): 87−115(in Chinese with English abstract).

中文参考文献

曹建劲,胡瑞忠,谢桂青,等,2009.广东沿海地区基性岩脉地球化学及成因.岩石学报,25(4):984−1000.

陈新跃,王岳军,韩会平,等,2014.琼西南三叠纪基性岩脉年代学、地球化学特征及其构造意义.吉林大学学报(地球科学版),44(3):835−847.

高维,施建荣,孟庆奎,等,2022.海南岛印支期麻粒岩的发现及其地质意义:来自锆石U-Pb定年与微量元素组成的新证据.地质学报,96(2):426−444.

葛小月,2003.海南岛中生代岩浆作用及其构造意义:年代学、地球化学及Sr-Nd同位素证据(博士学位论文).广州:中国科学院研究生院(广州地球化学研究所).

巩小栋,唐渊,秦雅东,等,2020.晚三叠世金沙江结合带碰撞作用:贡觉石英二长岩年代学、地球化学及Hf同位素证据.地球科学,45(8):2905−2919.

苟琪钰,钱鑫,何慧莹,等,2019.海南荔枝沟中三叠世酸性火山岩年代学、地球化学特征及其构造意义.地球科学,44(4):1357−1370

郝宇杰,任云生,史雨凡,等,2020.黑龙江省完达山地区河口林场斑岩型锡多金属矿床花岗斑岩的形成年代、岩石成因及构造背景.岩石学报,36(3):837−855.

胡林,熊富浩,陈安清,等,2024.琼东南盆地花岗质岩浆−构造演化及其对潜山储层物性的约束.地质通报,43(7):1191−1206.

胡瑞忠,毕献武,彭建堂,等,2007.华南地区中生代以来岩石圈伸展及其与铀成矿关系研究的若干问题.矿床地质,26(2):139−152.

解习农,张成,任建业,等,2011.南海南北大陆边缘盆地构造演化差异性对油气成藏条件控制.地球物理学报,54(12):3280−3291.

雷超,任建业,张静,2015.南海构造变形分区及成盆过程.地球科学,40(4):744−762.

李龚健,王庆飞,禹丽,等,2013.哀牢山古特提斯洋缝合时限:晚二叠世花岗岩类锆石U-Pb年代学与地球化学制约.岩石学报,29(11):3883−3900.

李慧玲,钱鑫,余小清,等,2023.越南昆嵩地体三叠纪花岗岩岩石成因及其特提斯构造意义.地球科学,48(4):1441−1460.

李三忠,索艳慧,周洁,等,2022.华南洋陆过渡带构造演化:特提斯构造域向太平洋构造域的转换过程与机制.地质力学学报,28(5):683−704.

李文庆,2019.硼酸盐熔融制样法测定辉绿岩中10种常量元素的准确度.世界地质,38(3):843−851.

刘飞,杨经绥,冯光英,等,2022.古太平洋板片晚二叠−早三叠世俯冲后撤:来自海南岛弧岩浆作用的制约.岩石学报,38(11):3455−3483.

刘晔,柳小明,胡兆初,等,2007.ICP-MS测定地质样品中37个元素的准确度和长期稳定性分析.岩石学报,23(5):1203−1210.

鲁宝亮,王璞珺,张功成,等,2015.南海区域断裂特征及其基底构造格局.地球物理学进展,30(4):1544−1553.

罗伟,彭静,金廷福,等,2023.川西李家沟锂多金属矿区晚三叠世花岗细晶岩脉的成因:地球化学、锆石U-Pb年龄和Hf同位素的证据.沉积与特提斯地质,43(1):36−47.

吕方,辛宇佳,李建华,等,2023.海南岛二叠纪—三叠纪构造演化:源自岩浆岩和变质岩同位素年代学和地球化学的

约束.地质学报,97(1):30－51.

吕昭英,陈沐龙,傅杨荣,等,2019.海南岛儋州地区两期A型花岗岩的岩石成因与地质意义.矿产与地质,(334):660－669.

毛建仁,厉子龙,叶海敏,2014.华南中生代构造－岩浆活动研究:现状与前景.中国科学:地球科学,44(12):2593－2617.

齐重向,温淑女,庞崇进,等,2023.海南岛北部中三叠世A型花岗岩的成因及其地质意义.地球化学,52(1):69－83.

施和生,杨计海,张迎朝,等,2019.琼东南盆地地质认识创新与深水领域天然气勘探重大突破.中国石油勘探,24(6):691－698

唐历山,朱继田,姚哲,等,2017.琼东南盆地松南低凸起潜山演化及成藏条件.特种油气藏,24(1):87－91.

唐立梅,陈汉林,董传万,等,2013.海南岛中三叠世造山后伸展作用:双峰式侵入岩的年代学及地球化学制约.中国科学:地球科学,43(3):433－445.

王瑜,2004.构造热年代学:发展与思考.地学前缘,11(4):435－443.

温淑女,梁新权,范蔚茗,等,2013.海南岛乐东地区志仲岩体锆石U-Pb年代学、Hf同位素研究及其构造意义.大地构造与成矿学,37(2):294－307.

吴福元,万博,赵亮,等,2020.特提斯地球动力学.岩石学报,36(6):1627－1674.

吴克强,解习农,裴健翔,等,2023.超伸展陆缘盆地深部结构及油气勘探意义:以琼东南盆地为例.石油与天然气地质,44(3):651－661.

谢才富,朱金初,丁式江,等,2006.海南尖峰岭花岗岩体的形成时代、成因及其与抱伦金矿的关系.岩石学报,22(10):2493－2508.

谢才富,朱金初,赵子杰,等,2005.三亚石榴霓辉石正长岩的锆石SHRIMP U-Pb年龄:对海南岛海西－印支期构造演化的制约.高校地质学报,11(1):47－57.

熊莉娟,李三忠,索艳慧,等,2012.南海南部新生代控盆断裂特征及盆地群成因.海洋地质与第四纪地质,32(6):113－127.

徐长贵,侯明才,吴克强,等,2024.琼东南盆地二叠纪－三叠纪长英质岩浆作用:对南海北部陆缘构造属性与演化过程的启示.岩石学报,40(8):2450－2468.

杨计海,黄保家,杨金海,2019.琼东南盆地深水区松南低凸起天然气成藏条件与勘探潜力.中国海上油气,31(2):1－10.

杨军,施小斌,王振峰,等,2015.琼东南盆地张裂期沉降亏损与裂后期快速沉降成因.海洋地质与第四纪地质,35(1):81－90

余金杰,陈福雄,王永辉,等,2012.海南石碌铁矿外围花岗岩类成因及形成的构造环境.中国地质,39(6):1700－1711.

张功成,米立军,吴景富,等,2010.凸起及其倾没端:琼东南盆地深水区大中型油气田有利勘探方向.中国海上油气,22(6):360－368.

张功成,杨东升,郭帅,等,2023.基岩潜山三元主导油气成藏模式:兼论南海北部深水区勘探新领域.天然气地球科学,34(12):2045－2061.

赵国锋,刘汇川,钱鑫,等,2018.琼东南晚二叠世Ⅰ型花岗岩成因及其构造指示.地球科学,43(4):1321－1332.

钟佳,王岩泉,2022.琼东南盆地松南低凸起花岗岩年代学、地球化学特征及构造环境.吉林大学学报(地球科学版),52(1):134－148.

周岱,胡军,杨文强,等,2021.粤西新兴岩体的形成时代与成因研究:对古特提斯洋东支关闭时间的约束.中国地质,48(6):1896－1923.

周凤娟,丁琳,李晓艳,等,2023.珠一坳陷文昌组锆石定年物源示踪及其对储层的影响.非常规油气,10(3):46－54.

周虎,付于真,胡潜伟,等,2024.琼东南盆地潜山晚三叠世辉绿岩的年代学、地球化学及其构造背景.成都理工大学学报(自然科学版),51(4):543－560.

周佐民,谢才富,徐倩,等,2011.海南岛中三叠世正长岩－花岗岩套的地质地球化学特征与构造意义.地质论评,57(4):515－531.

朱炳泉,1998.壳幔化学不均一性与块体地球化学边界研究.地学前缘,5(1):72－82.

祝嵩,姚永坚,李学杰,2021.南海及邻区岩浆岩时空分布特征及机制.海洋地质与第四纪地质,41(4):87－115.